ISS Method for Coordination Control of Nonlinear Dynamical Agents Under Directed Topology

Xiangke Wang *Member, IEEE,* Jiahu Qin *Member, IEEE,* Changbin Yu *Senior Member, IEEE*

***Abstract*—The problems of coordination of multiagent systems with second-order locally Lipschitz continuous nonlinear dynamics under directed interaction topology are investigated in this paper. A completely nonlinear input-to-state stability (ISS)-based framework, drawing on ISS methods, with the aid of results from graph theory, matrix theory, and the ISS cyclic-small-gain theorem, is proposed for the coordination problem under directed topology, which can effectively tackle the technical challenges caused by locally Lipschitz continuous dynamics. Two coordination problems, i.e., flocking with a virtual leader and containment control, are considered. For both problems, it is assumed that only a portion of the agents can obtain the information from the leader(s). For the first problem, the proposed strategy is shown effective in driving a group of nonlinear dynamical agents reach the prespecified geometric pattern under the condition that at least one agent in each strongly connected component of the information-interconnection digraph with zero in-degree has access to the state information of the virtual leader; and the strategy proposed for the second problem can guarantee the nonlinear dynamical agents moving to the convex hull spanned by the positions of multiple leaders under the condition that for each agent there exists at least one leader that has a directed path to this agent.**

***Index Terms*—Directed topology, ISS, locally lipschitz continue, multiagent coordination, second-order nonlinear dynamics.**

I. Introduction

OVER THE LAST few years, coordination control problems for multiagent systems have attracted considerable attentions from the control community, due to its broad range of applications in, for example, space missions, security patrols, search and rescue in hazardous environments [1]–[4].

Manuscript received July 2, 2012; revised August 27, 2013; accepted December 6, 2013. Date of publication January 9, 2014; date of current version September 12, 2014. This work was supported in part by the Research Project of National University of Defense Technology under Grant JC13-03-02, in part by the Program for New Century Excellent Talents in University (China) under Grant NCET-13-0544, in part by the NSFC under Grant 61375072, in part by the Grant ARC-DP130103610, in part by the Queen Elizabeth II Fellowship under Grant DP-110100538, and in part by the joint SDAS-ANU Grant, SDAS Pilot Project and the Overseas Expert Program of Shandong Province. This paper was recommended by Associate Editor J. Shamma.

X. Wang is with the College of Mechatronic Engineering and Automation, National University of Defense Technology, Changsha, 410073, China (e-mail: xkwang@nudt.edu.cn).

J. Qin is with University of Science and Technology of China, Hefei 230026, China, and also with the Australian National University, Canberra ACT 2601, Australia (e-mail: jiahu.qin@gmail.com).

C. Yu is with the Australian National University, Canberra ACT 2601, Australia and Shandong Computer Science Center (e-mail: brad.yu@anu.edu.au).

Color versions of one or more of the figures in this paper are available online at http://ieeexplore.ieee.org.

Digital Object Identifier 10.1109/TCYB.2013.2296311

Motivated by different fields such as biology and physics [5]–[7], one coordination control problem is flocking. The classical flocking model is proposed by Reynolds in [5] to describe the self-driven particle systems. Since then, many studies have been done on the flocking problem for agents modeled by double-integrator dynamics under undirected topology [8]–[10]. Few works have been considered for the flocking of agents modeled by nonlinear dynamics. It is worth noting that Dong proposed a backstepping-based control law design method for the flocking of multiple nonholonomic wheeled mobile robots communicating under directed topology in [11].

A similar problem considered in multiagent systems is consensus, in which all the states eventually reach an agreement (see [12] for a tutorial overview about topic). Most of the existing literature focuses on consensus algorithms for agents governed by linear dynamics, especially by the single- or double-integrator dynamics, [13]–[17], to name a few. The most common continuous-time consensus algorithm for the multiagent systems with single-integrator model is given by

$$\dot{x}_i = -\sum_{j=1}^{n} \alpha_{ij}(x_i - x_j), \quad i = 1, \dots, n \tag{1}$$

where x_i is the state of the ith agent and α_{ij} is the (i, j) entry of the adjacency matrix of the associated communication topology. When the communication topology is a directed graph without switching, protocol (1) can guarantee consensus if the communication graph has a rooted spanning tree. The results of single-integrator system have been extended to the consensus of double-integrator or high-order linear systems, and similar consensus protocols and graph conditions are obtained [18]–[22]. Consensus for multiagent systems with nonlinear dynamics has also received increasing attention in the past years, for example, in [23] and [24], where the continuously differentiable nonlinear dynamics are considered; in [25]–[27] where the nonlinear dynamics satisfies the global Lipschitz condition; and in [28] where an adaptive control method is introduced to study the synchronization of uncertain nonlinear networked systems.

Recently, a coordination extended from the flocking problem, named containment control, where the states of the followers are driven to the convex hull spanned by the states of multiple leaders, has also been investigated for coordinated agents governed by single- or double-integrator dynamics [29]–[34]. Of which, Li *et al.* [30] proposed two containment control algorithms via only position measurements where the leaders were neighbors of only a subset of the followers. Lou and Hong [31] considered the containment control for a second-order multiagent system with random switching topologies. Further, the containment control strategy for multiple Lagrangian system in directed topological structure was proposed in [32]; and the containment control of multiple rigid-body systems with uncertainty was studied in [33]. For the more general nonlinear dynamics, Shi *et al.* [34] investigated the distributed set tracking problem with unmeasurable velocities under switching directed topologies, and provided the necessary and sufficient conditions for set input-to-state stability and set integral input-to-state stability.

Since most of physical systems are inherently nonlinear in nature, it is necessary and beneficial to study multiagent coordination control, including flocking and containment control, in the presence of the nonlinearities. In this paper, we will investigate flocking with a virtual leader and containment control for nonlinear multiagent systems. However, different from all the above-mentioned works, the nonlinear dynamics considered in this paper is only required to be locally Lipschitz continuous, a rather relaxed assumption which has been used in a wide-range of practical nonlinear systems [35]. Naturally, such relaxed assumption will bring out more technical challenges than the nonlinear dynamics considered in the existing works [11], [25], [26], where various restrictive conditions are imposed on the nonlinear dynamics so that the nonlinear dynamics can be approximated by linear dynamics. This in turn makes the techniques performed in such works are in fact for linear systems, and thus cannot be extended to deal with the technical challenges caused by the locally Lipschitz continuous dynamics.

The key tool employed to tackle the challenge of locally Lipschitz continuous nonlinearity in this paper is the newly developed cyclic-small-gain theorem, which provides a frame and design method to guarantee the stability of the interconnected input-to-state stability (ISS) subsystems. The concept of ISS, aiming mainly at describing how external inputs affect the internal stability, has been widely used and investigated in nonlinear system community (see [36] for a tutorial). Recently, it has been further extended to analyze the stability of interconnected nonlinear systems [37], [38]. Dashkovskiy *et al.* [37] develop a matrix-small-gain criterion for networks with plus-type interconnections and mentioned the cyclic-small-gain condition, and an ISS-Lyapunov function based cyclic-small-gain theorem is presented in [38], in which it is proved that the nonlinear system composed of interconnected ISS subsystems is ISS if the cyclic-small-gain condition is satisfied. The cyclic-small-gain condition can be roughly described as follows: the composition of the gain functions along every cycle in the network of ISS systems is less than the identity function.

This paper provides a new approach, which is a blend of algebraic graph theory, ISS method especially the cyclic-small-gain theorem, and backstepping techniques, to deal with coordination problems under directed topology, in which each agent is governed by second-order locally Lipschitz continuous dynamics. Two focal coordination problems, i.e., flocking with a virtual leader and containment control, are investigated under directed topology via local interactions. The flocking behavior in this paper refers to that the position center of all agents approaches to a virtual leader with the prespecified geometric pattern and meanwhile the velocities of the agents converge to zero; while the containment control is that the positions of agents converge to the convex hull spanned by the positions of multiple stationary leaders. In the new approach, the closed-loop multiagent system is first transformed into a two-cascade model, and then by exploring the algebraic properties of the digraphs and designing a virtual control input for each subsystem in the two-cascade model, the ISS of the whole system can be guaranteed by the cyclic-small-gain theorem, which leads to the asymptotic stability of the coordination problems for the closed-loop multiagent systems. The contributions of this paper lie on four aspects. First, this paper provides a completely nonlinear ISS-based framework and analyzing method for the coordinated flocking and containment control problems under directed topology, which can effectively tackle the technical challenges caused by locally Lipschitz continuous dynamics. To the best of our knowledge, in most of the existing results on coordination problems of nonlinear systems, the dynamics of agents are confined to be continuously differentiable or globally Lipschitz continuous. Different from the existing works, the nonlinear dynamics considered in this paper is only required to be locally Lipschitz continuous, a rather relaxed condition which has been used in a wide range of practical nonlinear systems; and mostly importantly, the performed techniques in existing work cannot be extended to deal with such dynamics. In addition, the study shows that only a fraction of agents having access to the state information of the leader(s) under directed local interconnections can guarantee the coordinated behaviors. To be more specifical, the sole requirement for the control strategies is that at least one agent in each strongly connected component of the interconnection digraph with zero in-degree has access to the state information of the virtual leader for the flocking behavior or for each agent there exists at least one leader that has a directed path to this agent for the containment control. Third, it is also worth mentioning here that the used model applies the coordination control of heterogeneous or isomorphic agents since the nonlinear dynamics modeling the insolated agents are allowed to be different with each other. Moreover, for each agent, the new strategies only need the information of its position, velocity and the relative positions to its neighbors, without requiring its neighbors' velocities. Finally, by using the design methodology in this paper, we are able to extend many existing first-order results to the second-order, or even higher-order case with nonlinear dynamics, which is certainly nontrivial.

The rest of the paper is organized as follows. Section II provides the basic notions and results concerning matrix theory, graph theory, and the ISS cyclic-small-gain theorem, as well as some backgrounds about the locally Lipschitz continuous dynamics to be considered. The main contents, i.e., the control designs with numerical examples for flocking and containment control based on graph theory, matrix theory and cyclic-small-gain theorem, are elaborated in Sections III and IV, respectively. Finally, Section V draws the conclusions and proposes some future works.

II. Background and Preliminaries

In this section, we present some basic notions and results in matrix and graph theory [39]–[41], ISS concepts [36], [38], as well as the nonlinear dynamics modeling the agents.

A. Matrix and Graph

We use $|\cdot|$ to denote the Euclidean norm for vectors or the 2-norm for matrices, and $\|\cdot\|$ to denote the L_∞ norm for vectors and matrices, respectively. A vector that consists of all zero or one entries is denoted by $\mathbf{0}$ or $\mathbf{1}$, respectively. For a square matrix M, we denote by $M > 0$ that M is positive definite and by $M < 0$ that M is negative definite, respectively. For a column vector $m = \{m_1, \ldots, m_n\}^{\mathrm{T}} \in \mathbb{R}^n$, the notion $M = \mathrm{diag}\{m\}$ represents a diagonal matrix with m_i being the i-th $(i = 1, \ldots, n)$ diagonal entry. For notational economy, we employ $DSum\{Q\} \in \mathbb{R}^{m\times m}$ to denote the diagonal matrix with the ith $(i = 1, 2, \ldots, m)$ diagonal element being the ith row sum of matrix $Q \in \mathbb{R}^{m\times n}$. For example, given

$$Q = \begin{bmatrix} 1 & 2 & 3 \\ 0 & 1 & -2 \end{bmatrix},$$

we have

$$DSum\{Q\} = \begin{bmatrix} 6 & 0 \\ 0 & -1 \end{bmatrix}.$$

Lemma 1: (Schur Complement, [40]) Given constant matrices S_1, S_2 and S_3 where $S_1 = S_1^{\mathrm{T}}$ and $S_2 = S_2^{\mathrm{T}} > 0$. Then $S_1 - S_3^{\mathrm{T}} S_2^{-1} S_3 > 0$ if and only if

$$\begin{bmatrix} S_1 & S_3^{\mathrm{T}} \\ S_3 & S_2 \end{bmatrix} > 0 \quad \text{or} \quad \begin{bmatrix} S_2 & S_3 \\ S_3^{\mathrm{T}} & S_1 \end{bmatrix} > 0.$$

Lemma 2: ([41]) Let $L \in \mathbb{R}^{N\times N}$. Then, all eigenvalues of L have positive real parts if and only if there exists a $P > 0 \in \mathbb{R}^{N\times N}$ such that $PL + L^T P > 0$.

Definition 1: ([29]) Let $\mathcal{C}$ be a set in a real vector space $\mathcal{V} \subseteq \mathbb{R}^n$. The set $\mathcal{C}$ is called convex if, for any x and y in $\mathcal{C}$, the point $(1-t)x + ty \in \mathcal{C}$ for any $t \in [0, 1]$. The convex hull for a set of points $x = \{x_1, \ldots, x_N\}$ in $\mathcal{V}$ is the minimal convex set containing all points in x. We use $Co(x)$ to denote the convex hull of x. In particular, $Co(x) = \{\sum_{i=1}^N \alpha_i x_i | x_i \in x, \alpha_i \geq 0, \sum_{i=1}^N \alpha_i = 1\}$.

A digraph (or directed graph) will be used to model the information or gain interconnection for multiagent systems. Let $\mathcal{G} = (\mathcal{V}, \mathcal{E}, \mathcal{A})$ be a weighted digraph of order N with a finite nonempty set of nodes $\mathcal{V} = \{1, 2, \ldots, N\}$; a set of directed edges $\mathcal{E} \subseteq \mathcal{V} \times \mathcal{V}$; and a weighted adjacency matrix $A_{\mathcal{G}} = [\alpha_{ij}] \in \mathbb{R}^{N\times N}$ with nonnegative adjacency elements α_{ij}. The adjacency elements associated with the edges are positive, i.e., $(j, i) \in E \Leftrightarrow \alpha_{ij} > 0$. The degree matrix $\Delta_{\mathcal{G}} = [\Delta_{ij}]$ is a diagonal matrix with $[\Delta_{ii}] = \sum_{j=1}^N \alpha_{ij}$, $i = 1, \ldots, N$, being the in-degree of node i, and the Laplacian of weighted digraph $\mathcal{G}$ is defined by $L_{\mathcal{G}} = \Delta_{\mathcal{G}} - A_{\mathcal{G}}$.

A directed path in digraph $\mathcal{G}$ is a sequence of directed edges in $\mathcal{G}$ of the form $(i_1, i_2), (i_2, i_3), \ldots, (i_{l-1}, i_l)$. Further, if i_1 and i_l are coincided, i.e., $i_1 = i_l$, then it is a circle. A subgraph $\mathcal{H}$ is called a induced digraph of $\mathcal{G}$ if, for any pair of nodes i and j of $\mathcal{H}$, (i, j) is an edge of $\mathcal{H}$ if and only if (i, j) is an edge of $\mathcal{G}$. A digraph is called strongly connected if any two distinct nodes of the digraph can be connected through a directed path. The strongly connected components of a digraph are its maximal strongly connected subgraphs, while given a digraph $\mathcal{G}$, a strongly connected component, say $\mathcal{G}_s$, within $\mathcal{G}$ is called with zero in-degree means that there are no edges starting from a node outside component $\mathcal{G}_s$ but ending on a node in it. We say that a digraph has a spanning tree if there exists at least one node, called the root node, having a directed path to all the other nodes.

Lemma 3: ([41]) If digraph $\mathcal{G}$ with N nodes is strongly connected, then there exists a positive column vector $b = [b_1, b_2, \ldots, b_N]^T \in \mathbb{R}^N$ satisfying $b^{\mathrm{T}} L_{\mathcal{G}} = 0$ and $b^{\mathrm{T}}\mathbf{1} = 1$ with $b_i > 0$ for $i = 1, \ldots, N$, where $L_{\mathcal{G}}$ is the Laplacian of digraph $\mathcal{G}$.

B. ISS and Small-Gain Theorem

A function $\alpha : \mathbb{R}_+ \to \mathbb{R}_+$ is said to be positive definite if it is continuous, $\alpha(0) = 0$ and $\alpha(s) > 0$ for $s > 0$. A function $\gamma : \mathbb{R}_+ \to \mathbb{R}_+$ is of class $\mathcal{K}$ if it is continuous, strictly increasing and $\gamma(0) = 0$; it is of class $\mathcal{K}_\infty$ if, in addition, it is unbounded. A function $\beta : \mathbb{R}_+ \times \mathbb{R}_+ \to \mathbb{R}_+$ is of class $\mathcal{KL}$ if, for each fixed t, the function $\beta(\cdot, t)$ is of class $\mathcal{K}$ and, for each fixed s, the function $\beta(s, \cdot)$ is decreasing and tends to zero at infinity. For nonlinear functions γ_1 and γ_2 defined on $\mathbb{R}_+$, inequality $\gamma_1 \leq \gamma_2$ (or $\gamma_1 < \gamma_2$) represents $\gamma_1(s) \leq \gamma_2(s)$ (or $\gamma_1(s) < \gamma_2(s)$) for all $s > 0$. Id represents identify function, and symbol $\circ$ denotes the composition between functions. For a real-valued differentiable function V, ∇V stands for its gradient. A system with state y is called the y-system.

Consider the following nonlinear system with $x \in \mathbb{R}^n$ as the state and $w \in \mathbb{R}^m$ as the external input:

$$\dot{x} = f(x, w) \tag{2}$$

where $f : \mathbb{R}^n \times \mathbb{R}^m \to \mathbb{R}^n$ is a locally Lipschitz vector field.

Definition 2 ([36]): The system (2) is said to be ISS with w as input if there exist $\beta \in \mathcal{KL}$ and $\gamma \in \mathcal{K}$ such that, for each initial condition $x(0)$ and each measurable essentially bounded input $w(\cdot)$ defined on $[0, \infty)$, the solution $x(\cdot)$ exists on $[0, \infty)$ and satisfies $|x(t)| \leq \beta(|x(0)|, \gamma(\|w\|))$, $\forall t \geq 0$.

It is known that if the system $\dot{x} = f(x, w)$ in (2) is ISS with w as the input, then the unforced system $\dot{x} = f(x, 0)$ is globally asymptotically stable at $x = 0$ [36].

Definition 3 ([36]): For a nonlinear system (2) with state $x \in \mathbb{R}^n$ and external input $w \in \mathbb{R}^m$, a function V is said to be an ISS-Lyapunov function if it is differentiable almost everywhere, and satisfies that

1) V is positive definite and radially unbounded, that is, there exist $\underline{\alpha}, \overline{\alpha} \in \mathcal{K}_\infty$ such that

$$\underline{\alpha}(|x|) \leq V(x) \leq \overline{\alpha}(|x|), \quad \forall x \in \mathbb{R}^n$$

2) there exists a positive definite α, and $\gamma \in \mathcal{K}$ such that

$$V(x) \geq \gamma(|w|) \Rightarrow \nabla V(x) f(x, w) \leq -\alpha(V(x)),$$
$$\forall x \in \mathbb{R}^n, \ \forall w \in \mathbb{R}^m.$$

Lemma 4 ([36]): The system (2) is ISS if and only if it has an ISS-Lyapunov function.

Consider the following interconnected system composed of N interacting subsystems:

$$x_i = f_i(x, w_i), \quad i = 1, \ldots, N \tag{3}$$

where $x_i \in \mathbb{R}^{n_i}$, $w_i \in \mathbb{R}^{m_i}$ and $f_i : \mathbb{R}^{n+m_i} \to \mathbb{R}^{n_i}$ with $n = \sum_{i=1}^{N} n_i$ is locally Lipschitz continuous such that $x = [x_1^T, \ldots, x_N^T]^T$ is the unique solution of system (3) for a given initial condition. The external input $w = [w_1^T, \ldots, w_N^T]^T$ is a measurable and locally essentially bounded function from $\mathbb{R}_+$ to $\mathbb{R}^m$ with $m = \sum_{i=1}^{N} m_i$. Further, we use γ_y^x to represent the gain from x-subsystem to y-subsystem.

Lemma 5 (Cyclic-Small-Gain Theorem, [38]): Consider the continuous-time dynamical network (3). Suppose that for the i-th ($i = 1, \ldots, N$) subsystem, there exists an ISS-Lyapunov function $V_i : \mathbb{R}^{n_i} \to \mathbb{R}$ satisfying

1) there exist $\underline{\alpha}_i, \overline{\alpha}_i \in \mathcal{K}_\infty$ such that

$$\underline{\alpha}_i(|x_i|) \le V_i(x_i) \le \overline{\alpha}_i(|x_i|), \quad \forall x_i \tag{4}$$

2) there exist $\gamma_{x_i}^{x_j} \in \mathcal{K} \cup \{0\}(j \neq i)$, $\gamma_{x_i}^{w_i} \in \mathcal{K} \cup \{0\}$ and a positive definite α_i such that

$$V_i(x_i) \ge \max\{\gamma_{x_i}^{x_j}(V_j(x_j)), \gamma_{x_i}^{w_i}(|w_i|)\}$$
$$\Rightarrow \nabla V_i(x_i) f_i(x_1, \ldots, x_N, w_i) \le -\alpha_i(V_i(x_i)) \ \forall x, \forall w_i. \tag{5}$$

Then, the system (3) is ISS if for each $r = 2, \ldots, N$

$$\gamma_{x_{i_1}}^{x_{i_2}} \circ \gamma_{x_{i_2}}^{x_{i_3}} \circ \cdots \circ \gamma_{x_{i_r}}^{x_{i_1}} < \mathrm{Id}$$

for all $1 \le i_j \le N$, $i_j \neq i_{j'}$ if $j \neq j'$.

C. Locally Lipschitz Continuous Dynamics

In this paper, we consider a group of N agents. For $i = 1, \ldots, N$, the dynamics of the ith agent is represented by

$$\dot{x}_i = v_i, \tag{6}$$
$$\dot{v}_i = f_i(x_i, v_i) + \mu_i, \tag{7}$$

where $x_i \in \mathbb{R}^n$ is the position, $v_i \in \mathbb{R}^n$ is the velocity, $\mu_i \in \mathbb{R}^n$ is the control input, and $f_i : \mathbb{R}^n \times \mathbb{R}^n \to \mathbb{R}^n$ is a locally Lipschitz continuous function, which is used to describe the nonlinear dynamics of the isolated agent.

Assumption 1: For each $i = 1, \ldots, N$, there exist $\psi_{f_i}^{x_i}$ and $\psi_{f_i}^{v_i} \in \mathcal{K}_\infty$ such that

$$|f_i(x_i, v_i)| \le \psi_{f_i}^{x_i}(|x_i|) + \psi_{f_i}^{v_i}(|v_i|). \tag{8}$$

Remark 1: Dynamics (6)–(7) with Assumption 1 is a normal model for the system with locally Lipschitz continuous dynamics, and widely used in the nonlinear control community [35]. If the term f_i does not exist, then the dynamics (6)–(7) is reduced to the widely studied double-integrator model [8]–[10], [19], [20]. However, to the best of our knowledge, few of the existing literature investigating multiagent distributed coordination control take the locally Lipschitz nonlinear dynamics, into account. For example, in [23] and [24], the nonlinear term f is assumed to be continuously differentiable, and in [25] and [26], f is assumed to be globally Lipschitz. Clearly, the nonlinear term $f_i(x_i, v_i)$ in (7) is not confined to be continuously differentiable or globally Lipschitz, and Assumption 1 is a rather relaxed assumption compared with the dynamics in most existing works. Further, it is worth pointing out here that the nonlinear term f_i in (7) is not required to be identical, which thus makes it valid to include more general cases such as coordination of heterogeneous or isomorphic agents into our framework.

III. Flocking With a Virtual Leader

In this section, we will design a control law to make the position center of the N agents follow a virtual leader $x_d \in \mathbb{R}^n$, meanwhile the positions of the N agents converge to a prespecified geometric pattern $\mathcal{P}$ from arbitrary initial positions and the velocities of all the agents converge to zero.

A. System Description

Similar to that used in [11], the geometric pattern is described by a tuple of N vectors, saying $\mathcal{P} = \{p_1, \ldots, p_N)$ with $p_i \in \mathbb{R}^n$; and further, without loss of generality, it is assumed that $\sum_{i=1}^{N} p_i = \mathbf{0}$ i.e., the center of the geometric pattern $\mathcal{P}$ is at the origin of the orthogonal coordinate system.

Remark 2: Note that the geometric pattern is used to represent the desired geometric shape of the positions of N agents relative to the virtual leader, which is a relative configuration, rather than a global information. In another words, the desired position center of the N agents is x_d, and the desired geometric shape of the positions of N agents is the geometric pattern $\mathcal{P}$ centered at x_d in the global coordination.

It is worthwhile to mention that the flocking or consensus problem with a virtual leader becomes much more complex if only a portion of the agents in the group have access to the virtual leader. However, in some nature examples, it is known that the movements, such as leading to the food source, of some animals, e.g., shoal, can be controlled by a few leaders [6], [7]. This gives rise to a new question naturally: which individuals should be informed to guarantee the stability of the movements in an arbitrarily given topological structure? In [8], all agents in the group are informed, i.e., all agents have access to the virtual leader; and in [9], it is proven that only a fraction of agents are informed can also cause flocking in the undirected topology, but without discussing which agents should be informed or the least agents which can be informed to guarantee the flocking. We consider also in this section the case that only a small part of the agents have access to the leader but under directed communication topology.

Denote the position center of N agents by $x_c = \frac{1}{N}\sum_{i=1}^{N} x_i$. The control objective here is to design a distributed control law for the ith agent in the form of $\mu_i = g_i(X_i)$ with

$$\begin{cases} \{x_i, v_i\} \cup \{x_j - x_i | j \in N_i\} \cup x_d, \\ \quad \text{if } x_d \text{ is available for the } i\text{th agent;} \\ \{x_i, v_i\} \cup \{x_j - x_i | j \in N_i\}, \\ \quad \text{if } x_d \text{ is not available for the } i\text{th agent;} \end{cases}$$

such that the position evolutions of the agents described by (6)–(7) asymptotically reach the geometric pattern $\mathcal{P}$, i.e.

$$\lim_{t\to\infty} |x_j(t) - x_i(t) - (p_j - p_i)| = 0 \tag{9}$$

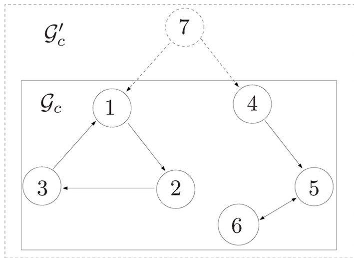

Fig. 1. $\mathcal{G}_c$ and $\mathcal{G}_c'$ of six-agent system. Nodes $i = \{1, \ldots, 6\}$ represent the ith agent and node 7 represents the virtual leader.

for $i, j = 1, \ldots, N$, and meanwhile the position center x_c converges to the virtual leader, i.e.

$$\lim_{t\to\infty} x_c(t) = x_d \tag{10}$$

and the velocities of all agents asymptotically converge to zero, i.e.

$$\lim_{t\to\infty} v_i(t) = 0. \tag{11}$$

B. Control Law Design

In the sequel, we will develop a nonlinear control law based on the graph theory, matrix theory and ISS cyclic-smaill-gain theorem to drive the N agents achieving (9)–(11).

1) *Two-Cascade Model:* Denote by $\mathcal{G}_c$, called the information-interconnection digraph, the digraph modeling the information interconnections among the N agents. Further, similar to that in [11] and [42], the virtual leader x_d is treated as a node indexed $N+1$. Define $\mathcal{G}_c'$, termed as the virtual information-interconnection digraph, as the digraph consisting of $\mathcal{G}_c$, node $N+1$ and the directed edges from node $N+1$ (namely, the virtual leader) to those agents in $\mathcal{G}_c$ which have access to the state information of the virtual leader. To illustrate the notions of $\mathcal{G}_c$ and $\mathcal{G}_c'$ clearly, we give an example of six-agent system, shown in Fig. 1.

For $i = 1, \ldots, N$, we define

$$\bar{x}_i = x_i - p_i - x_d. \tag{12}$$

Correspondingly, we have

$$\dot{\bar{x}}_i = \dot{x}_i = v_i. \tag{13}$$

Denote $\bar{x} = [\bar{x}_1^T, \ldots, \bar{x}_N^T]^T$ and $v = [v_1^T, \ldots, v_N^T]^T$. From (13), we obtain

$$\dot{\bar{x}} = v. \tag{14}$$

Taking v as the virtual control input of the $\bar{x}$-subsystem in (14), for $i = 1, \ldots, N$, we define

$$v_i^* = -a_i\bar{x}_i + \sum_{j\in N_i} \alpha_{ij}(\bar{x}_j - \bar{x}_i) \tag{15}$$

where α_{ij} is the ijth element of the weighted adjacency matrix of $\mathcal{G}_c$; $a_i > 0 \in \mathbb{R}$ if the ith agent has access to the virtual leader and $a_i = 0$ otherwise.

Denote $z = [z_1^T, \ldots, z_N^T]^T$, $v^* = [v_1^{*T}, \ldots, v_N^{*T}]^T$ and $a = [a_1, \ldots, a_N]$. Then, from (15), we have

$$v^* = -\left(L_{\mathcal{G}_c} \otimes I_n\right)\bar{x} - (\mathrm{diag}\{a\} \otimes I_n)\,\bar{x}, \tag{16}$$

where $L_{\mathcal{G}_c}$ is the Laplacian of $\mathcal{G}_c$ and $\otimes$ is the Kronecker product between matrices.

Let $z = v - v^*$, it then follows directly from (14) and (16) that

$$\dot{\bar{x}} = z - \left(L_{\mathcal{G}_c} \otimes I_n\right)\bar{x} - (\mathrm{diag}\{a\} \otimes I_n)\,\bar{x}. \tag{17}$$

Differentiating both sides of (16), we have

$$\dot{v}^* = -\left(L_{\mathcal{G}_c} \otimes I_n\right)\dot{\bar{x}} - (\mathrm{diag}\{a\} \otimes I_n)\,\dot{\bar{x}}. \tag{18}$$

By substituting $\dot{\bar{x}}$ in (17) into (18) yields

$$\dot{v}^* = -\left\{(L_{\mathcal{G}_c} + \mathrm{diag}\{a\}) \otimes I_n\right\} z + \left\{(L_{\mathcal{G}_c} + \mathrm{diag}\{a\})^2 \otimes I_n\right\}\bar{x}. \tag{19}$$

Then, differentiating both sides of $z = v - v^*$ and using (19), we have

$$\dot{z} = \dot{v} + \left\{(L_{\mathcal{G}_c} + \mathrm{diag}\{a\}) \otimes I_n\right\} z - \left\{(L_{\mathcal{G}_c} + \mathrm{diag}\{a\})^2 \otimes I_n\right\}\bar{x}. \tag{20}$$

Consequentially, for $i = 1, \ldots, N$, by using (6) and (7), together with (17) and (20), the two-cascade model is summarized as follows:

$$\dot{\bar{x}} = z - \left\{(L_{\mathcal{G}_c} + \mathrm{diag}\{a\}) \otimes I_n\right\}\bar{x} \tag{21}$$

$$\begin{aligned}\dot{z}_i = {} & f_i(x_i, v_i) + \mu_i + (a_i + \sum_{j\in N_i}\alpha_{ji})z_i - \sum_{j\in N_i}\alpha_{ji}z_j \\ & - \left\{(L_{\mathcal{G}_c} + \mathrm{diag}\{a\})_i^2 \otimes I_n\right\}\bar{x}\end{aligned} \tag{22}$$

where $(L_{\mathcal{G}_c} + \mathrm{diag}\{a\})_i^2$ is the i-th row of $(L_{\mathcal{G}_c} + \mathrm{diag}\{a\})^2$. Note that cascade 1 described by (21) is a $\bar{x}$-subsystem, and cascade 2 described by (22) are z_i-subsystems.

2) *Cyclic-Small-Gain Conditions:* Consider the two-cascade model (21) and (22). Obviously, the $\bar{x}$-subsystem and z_i-subsystems are interconnected. Considering the states $\bar{x}$ and z_i as $N+1$ different nodes, and the gain connections between these states as directed edges, the interconnected $[\bar{x}^T, z_1^T, \ldots, z_N^T]^T$-system composed of the $\bar{x}$-subsystem and the z_i-subsystems can be modeled by a digraph $\mathcal{G}_g$, called the gain-interconnection digraph. Fig. 2 is the corresponding gain-interconnection digraph $\mathcal{G}_g$ of the information-interconnection digraph in Fig. 1. Note that the digraph induced from $\mathcal{G}_g$ with node set $\{1, 2, \ldots, N\}$ has the same topological structure with digraph $\mathcal{G}_c$. In fact, digraph $\mathcal{G}_g$ can be constructed from digraph $\mathcal{G}_c$ by adding one node (the node indexed by $\bar{x}$ in Fig. 2) together with $2N$ directed edges $(\bar{x}, z_i)$ and $(z_i, \bar{x})$ for $i = 1, \ldots, N$.

For notional convenience, we denote the nodes in $\mathcal{G}_c$ and the nodes representing the z_i-subsystems in $\mathcal{G}_g$ by $1, \ldots, N$, denote the additional node representing the $\bar{x}$-subsystem in $\mathcal{G}_g$ by $N+1$.

Based on the newly defined $\mathcal{G}_c$ and $\mathcal{G}_g$, we reinvestigate the cyclic-small-gain conditions required by Lemma 5, which can be explicitly described as follows:

$$L_{\mathcal{G}_c} = \begin{bmatrix} L_{11} + DSum\{L_{10}\} & 0 & \dots & 0 \\ L_{21} & L_{22} + DSum\{L_{20}\} & \dots & 0 \\ \vdots & \vdots & \ddots & \vdots \\ L_{q1} & L_{q2} & \ddots & L_{qq} + DSum\{L_{q0}\} \end{bmatrix}. \tag{30}$$

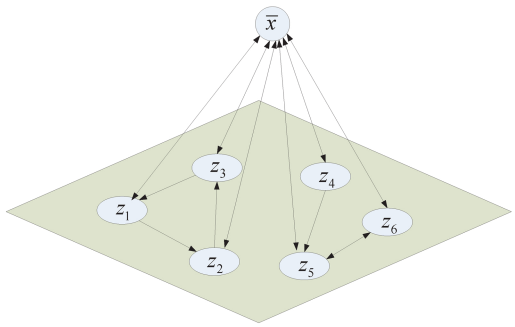

Fig. 2. Gain-interconnection digraph of six-agent system. Nodes z_i for $i = \{1, \dots, 6\}$ represent the z_i-subsystems and node $\bar{x}$ represents the $\bar{x}$-subsystem.

1) for each node i in $\mathcal{G}_c$, there exists a cycle $(i, N+1, i)$ in $\mathcal{G}_g$. The corresponding cyclic-small-gain condition is

$$\gamma_{z_i}^{\bar{x}} \circ \gamma_{\bar{x}}^{z_i} < \mathrm{Id} \tag{23}$$

2) for each directed path $(i_1, i_2, \dots, i_r)$ $(r \geq 2)$ in $\mathcal{G}_c$, [1] there exists a cycle $(i_1, \dots, i_r, N+1, i_1)$ in $\mathcal{G}_g$. The corresponding cyclic-small-gain condition is

$$\gamma_{z_{i_1}}^{z_{i_2}} \circ \gamma_{z_{i_2}}^{z_{i_3}} \circ \dots \circ \gamma_{z_{i_r}}^{\bar{x}} \circ \gamma_{\bar{x}}^{z_{i_1}} < \mathrm{Id} \tag{24}$$

3) for each directed cycle $(i_1, i_2, \dots, i_{c-1}, i_c, i_1)$ in $\mathcal{G}_c$, there also exists a cycle $(i_1, i_2 \dots, i_{c-1}, i_c, i_1)$ in $\mathcal{G}_g$. The corresponding cyclic-small-gain condition is

$$\gamma_{z_{i_1}}^{z_{i_2}} \circ \gamma_{z_{i_2}}^{z_{i_3}} \circ \dots \circ \gamma_{z_{i_{c-1}}}^{z_{i_c}} \circ \gamma_{z_{i_c}}^{z_{i_1}} < \mathrm{Id}. \tag{25}$$

Remark 3: In fact, the inequalities (23)–(25) can be guaranteed simply by choosing

$$\gamma_{z_j}^{z_i} < \mathrm{Id}, \quad (i, j) \in E \tag{26}$$

$$\gamma_{z_i}^{\bar{x}} = \gamma_{z_j}^{\bar{x}} < (\gamma_{\bar{x}}^{z_i})^{-1} = (\gamma_{\bar{x}}^{z_j})^{-1}, \quad 1 \leq i \neq j \leq N. \tag{27}$$

Obviously, the cyclic-small-gain conditions from (23) to (25) can be guaranteed by choosing (26) and (27) regardless of the number of the agents.

3) *Main Result:* Without loss of generality, we shall assume that $\mathcal{G}_c$ has q $(1 \leq q \leq N)$ strongly connected components, say $\mathcal{G}_1, \dots, \mathcal{G}_q$, respectively, and also $L_{\mathcal{G}'_c}$ takes the following Frobenius normal form [43]

$$L_{\mathcal{G}'_c} = \begin{bmatrix} L_{00} = 0 & 0 & 0 & \dots & 0 \\ L_{10} & L_{11} & 0 & \dots & 0 \\ L_{20} & L_{21} & L_{22} & \dots & 0 \\ \vdots & \vdots & \vdots & \ddots & \vdots \\ L_{q0} & L_{q1} & L_{q2} & \ddots & L_{qq} \end{bmatrix}. \tag{28}$$

[1]if $r = 2$, the directed path is a directed edge in $\mathcal{G}_c$.

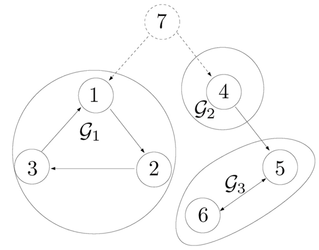

Fig. 3. Strongly connected components of $\mathcal{G}_c$ in Fig. 1, in which $\mathcal{G}_l$ $(l = 1, 2, 3)$ means the lth strongly connected component.

Recall that $a_i > 0$ for $i = 1, \dots, N$ if the ith agent has access to the state information of the virtual leader and $a_i = 0$ otherwise. It follows straightforwardly that

$$-[L_{10}^{\mathrm{T}}, L_{20}^{\mathrm{T}}, \dots, L_{q0}^{\mathrm{T}}] = [a_1, \dots, a_N]. \tag{29}$$

An example is given as Fig. 3, in which the strongly connected components of $\mathcal{G}_c$ in Fig. 1 are labeled.

In the sequel, we first investigate some algebraical properties of $\mathcal{G}'_c$, which will be used in the stability analysis of the flocking law, and then propose the main result on flocking problem.

The following result can be obtained by employing exactly the same proof as that in Lemma 4 in [42]. Hence, we omit its proof.

Lemma 6: If $\mathcal{G}'_c$ has a spanning tree, then for any $l = 2, \dots, q$, there exists a positive column vector $b_l \in \mathbb{R}^{n_l}$ such that the matrix $\mathrm{diag}\{b_l\} L_{ll} + L_{ll}^{\mathrm{T}} \mathrm{diag}\{b_l\} > 0$. In fact, b_l can be chosen as the positive left eigenvector of $L_{ll} + \sum_{i=1}^{l-1} DSum\{L_{li}\}$ associated with eigenvalue 0 satisfying $b_l^T \mathbf{1}_{n_l} = 1$ for $l = 2, \dots, q$.

According to Lemma 6, we can then obtain the following useful lemma.

Lemma 7: If digraph $\mathcal{G}'_c$ has a spanning tree, then there exists a positive column vector $c = [c_1, c_2, \dots, c_N]^{\mathrm{T}} \in \mathbb{R}^N$ such that $\hat{L}_{ca} = \frac{1}{2}[\mathrm{diag}\{c\}(L_{\mathcal{G}_c} + \mathrm{diag}\{a\}) + (L_{\mathcal{G}_c} + \mathrm{diag}\{a\})^{\mathrm{T}} \mathrm{diag}\{c\}] > 0$, where $L_{\mathcal{G}_c}$ is the Laplacian of the corresponding $\mathcal{G}_c$. Moreover, denote the smallest eigenvalue of $\hat{L}_{ca}$ by $\lambda_{\min}(\hat{L}_{ca})$, we have $x^{\mathrm{T}} \hat{L}_{ca} x \geq \lambda_{\min}(\hat{L}_{ca}) x^T x$ for any $x \in \mathbb{R}^N$.

Proof: It can be easily seen that the Laplacian of $\mathcal{G}_c$ can be represented by (30) (at the top of this page) from the definition of $\bar{\mathcal{G}}_c$ and (28).

And then $L_{\mathcal{G}_c}$ in (30), together with (29), imply that

$$L_{\mathcal{G}_c} + \mathrm{diag}\{a\} = \begin{bmatrix} L_{11} & 0 & \dots & 0 \\ L_{21} & L_{22} & \dots & 0 \\ \vdots & \vdots & \ddots & \vdots \\ L_{q1} & L_{q2} & \ddots & L_{qq} \end{bmatrix}.$$

On the other hand, noticing from Lemma 6 that there exists a positive column vector b_l such that $\mathrm{diag}\{b_l\}L_{ll}+L_{ll}^{\mathrm{T}}\mathrm{diag}\{b_l\} > 0$ holds for any $l = 2, \ldots, q$. Let $c = [b_1^T, \delta_2 b_2^{\mathrm{T}}, \ldots, \delta_q b_q^{\mathrm{T}}]^{\mathrm{T}}$, where δ_l for $l = 2, \ldots, q$ are positive numbers. In what follows, we will prove that there exists such $\delta_l > 0$ for $l = 2, \ldots, q$ that $\hat{L}_{ca} > 0$.

Let $\Phi_1 = \mathrm{diag}\{b_1\}L_{11} + L_{11}^{\mathrm{T}}\mathrm{diag}\{b_1\}$ and Φ_l defined in (31) (at the top of next page) for $l = 2, \ldots, q$. Note that $\Phi_q = \mathrm{diag}\{c\}(L_{\mathcal{G}_c} + \mathrm{diag}\{a\}) + (L_{\mathcal{G}_c} + \mathrm{diag}\{a\})^T\mathrm{diag}\{c\}$ and thus to complete the proof for the theorem, it suffices to prove that $\Phi_q > 0$ can be guaranteed if δ_l for $l = 2, \ldots, q$ are appropriately chosen. We will prove this argument by induction.

From Lemma 6, we know that $\Phi_1 > 0$. Supposed that when $l = k$, $2 \le k \le l$, there exists positive number δ_k such that $\Phi_k > 0$. Note also that $\mathrm{diag}\{b_{k+1}\}L_{k+1,k+1} + L_{k+1,k+1}^T\mathrm{diag}\{b_{k+1}\} > 0$ from Lemma 6, it then follows from Lemma 1 that $\Phi_{k+1} > 0$ if the following inequality

$$\begin{aligned}\Phi_k - \delta_{k+1}\Pi_{k+1}^T(&\mathrm{diag}\{b_{k+1}\}L_{k+1,k+1}\\ &+L_{k+1,k+1}^T\mathrm{diag}\{b_{k+1}\})^{-1}\Pi_{k+1} > 0\end{aligned} \tag{32}$$

where

$$\Pi_{k+1} = \left[\mathrm{diag}\{b_{k+1}\}L_{k+1,1} \cdots \mathrm{diag}\{b_{k+1}\}L_{k+1,k}\right]$$

holds. The inequality in (32) can be guaranteed by choosing any positive δ_{k+1} satisfying that Π_{k+1} is sufficiently smaller than Π_j for any $j \le k$. So, we completes the proof for the first statement.

The second statement can be obtained straightforwardly from the first statement. ■

Remark 4: It should be noted that in the proof of Lemma 7, and together with Lemma 3, the construction of the positive column vector $c = [b_1, \delta_2 b_2, \ldots, \delta_N b_N]^T \in \mathbb{R}^N$ is provided. Note that $L_{ll}+\sum_{i=1}^{l-1} DSum\{L_{li}\}$ is exactly the Laplacian of the lth strongly connected component of $\mathcal{G}_c$. Therefore, we first obtain all the strongly connected components of $\mathcal{G}_c$, denoted by $\mathcal{G}_1, \ldots, \mathcal{G}_q$, and obtain the Laplacian $L_{\mathcal{G}_l}$ ($l = 1, \ldots, q$) for each component, respectively. Then, b_l is the positive left eigenvector of $L_{\mathcal{G}_l}$ associated with eigenvalue 0 satisfying $b_l^T\mathbf{1}_{n_l} = 1$. Consequently, δ_{l+1} ($l = 1, \ldots, q-1$) can be chosen to guarantee (32) hold. Finally, combining all the b_l and δ_l, the positive column vector c is obtained.

Denote $c_{\min} = \min\{c_1, \ldots, c_N\}$, $c_{\max} = \max\{c_1, \ldots, c_N\}$ and $\hat{L}_{2a} = \frac{1}{2}\left((L_{\mathcal{G}_c} + \mathrm{diag}\{a\})^2 + (L_{\mathcal{G}_c}^{\mathrm{T}} + \mathrm{diag}\{a\})^2\right)$. Based on the cyclic-small-gain theorem, the gain-interconnection digraph and Lemma 7, we now can provide the first main result.

Theorem 1: For a group of N agents with dynamics (6)–(7) satisfying Assumption 1, if $\mathcal{G}_c'$ has a spanning tree, and the cyclic-small-gain conditions (23)–(25) resulting from its corresponding $\mathcal{G}_g$ hold, then control law

$$\mu_i = \begin{cases} -\frac{z_i}{|z_i|}\mu_i' - \left(\frac{\sigma_{z_i}}{2} + a_i + \sum_{j\in N_i}\alpha_{ji}\right)z_i, & \text{when } z_i \ne 0\\ 0, & \text{when } z_i = 0\end{cases} \tag{33}$$

where

$$\mu_i' = \psi_{f_i}^{x_i}(|x_i|) + \psi_{f_i}^{v_i}(|v_i|) + |\hat{L}_{2a_i}|\rho_{\bar{x}}^{z_i}(|z_i|) + \sum_{j\in N_i}\alpha_{ji}\rho_{z_j}^{z_i}(|z_i|)$$

and $\hat{L}_{2a_i}$ is the ith row of $\hat{L}_{2a}$, $\sigma_{z_i} > 0$ is an arbitrary positive real constant, $\rho_{\bar{x}}^{z_i}(s) = \tau^{-1} \circ \left(\gamma_{z_i}^{\bar{x}}\right)^{-1} \circ c_{\min}^{-1} \circ \tau(s)$ and $\rho_{z_j}^{z_i}(s) = \tau^{-1} \circ \left(\gamma_{z_i}^{z_j}\right)^{-1} \circ \tau(s)$ with functions $\gamma_{z_i}^{\bar{x}}$ and $\gamma_{z_i}^{z_j}$ for $j \in N_i$ are any functions of class $\mathcal{K}_\infty$ and $\tau(s) = \frac{1}{2}s^2$, can guarantee the flocking of N agents finally, namely the objective described by (9)–(11) is achieved.

Proof: We define the ISS-Lyapunov function candidates for the $\bar{x}$-subsystem and z_i-subsystems, respectively, as follows:

$$V_{\bar{x}}(\bar{x}) = \frac{1}{2}\bar{x}^{\mathrm{T}}(\mathrm{diag}\{c\} \otimes I_n)\bar{x} \tag{34}$$

$$V_{z_i}(z_i) = \tau(|z_i|), \quad i = 1, \ldots, N. \tag{35}$$

In the following discussions, $V_{\bar{x}}$ and V_{z_i} are simply used instead of $V_{\bar{x}}(\bar{x})$ and $V_{z_i}(z_i)$, respectively.

Taking the derivative of $V_{\bar{x}}$ defined in (34), and then using (21), we have

$$\begin{aligned}\nabla V_{\bar{x}}\dot{\bar{x}} &= \frac{1}{2}\left(\dot{\bar{x}}^T(\mathrm{diag}\{c\} \otimes I_n)\bar{x} + \bar{x}^T(\mathrm{diag}\{c\} \otimes I_n)\dot{\bar{x}}\right)\\ &= -\bar{x}^T(\hat{L}_{ca} \otimes I_n)\bar{x} + \frac{1}{2}z^T\mathrm{diag}\{c\}\bar{x} + \frac{1}{2}\bar{x}^T\mathrm{diag}\{c\}z.\end{aligned}$$

As $\mathcal{G}_c'$ has a spanning tree, from Lemma 7, it is obtained that $\hat{L}_{ca} > 0$, and further $\nabla V_{\bar{x}}\dot{\bar{x}}$ yields

$$\nabla V_{\bar{x}}\dot{\bar{x}} \le -\lambda_{\min}(\hat{L}_{ca})|\bar{x}|^2 + |diag\{c\}||\bar{x}||z|.$$

As vector c is positive, we have $|\mathrm{diag}\{c\}| = c_{\max}$, and

$$\nabla V_{\bar{x}}\dot{\bar{x}} \le -\lambda_{\min}(\hat{L}_{ca})|\bar{x}|^2 + c_{\max}|\bar{x}||z|. \tag{36}$$

Considering any positive $0 < \epsilon < \lambda_{\min}(\hat{L}_{ca})$, we define a function of class $\mathcal{K}_\infty$ as

$$\gamma_{\bar{x}}^{z_i}(s) = Nc_{\max}\left(\frac{c_{\max}}{\lambda_{\min}(\hat{L}_{ca}) - \epsilon}\right)^2 s, \quad \forall s \in \mathbb{R}_+.$$

When $V_{\bar{x}} \ge \max_{i=1,\ldots,N}\left\{\gamma_{\bar{x}}^{z_i}(V_{z_i})\right\}$, we have

$$\begin{aligned}\frac{1}{2}c_{\max}|\bar{x}|^2 \ge V_{\bar{x}} &\ge c_{\max}\left(\frac{c_{\max}}{\lambda_{\min}(\hat{L}_{ca}) - \epsilon}\right)^2\sum_{i=1}^N V_{z_i}\\ &= \frac{1}{2}c_{\max}\left(\frac{c_{\max}}{\lambda_{\min}(\hat{L}_{ca}) - \epsilon}\right)^2 z^T z\end{aligned}$$

which implies

$$|z| \le \frac{(\lambda_{\min}(\hat{L}_{ca}) - \epsilon)}{c_{\max}}|\bar{x}|. \tag{37}$$

Substituting (37) into (36), it is achieved $\nabla V_{\bar{x}}\dot{\bar{x}} \le -\epsilon|\bar{x}|^2 \le -\frac{2\epsilon}{c_{\max}}V_{\bar{x}}$. Therefore, we conclude $V_{\bar{x}}$ satisfying

$$V_{\bar{x}} \ge \max_{i=1,\ldots,N}\left\{\gamma_{\bar{x}}^{z_i}(V_{z_i})\right\} \Rightarrow \nabla V_{\bar{x}}\dot{\bar{x}} \le -\frac{2\epsilon}{c_{\max}}V_{\bar{x}}. \tag{38}$$

$$\Phi_l = \begin{bmatrix} \mathrm{diag}\{b_1\}L_{11} + L_{11}^{\mathrm{T}}\mathrm{diag}\{b_1\} & \delta_2 L_{21}^{\mathrm{T}}\mathrm{diag}\{b_2\} & \cdots & \delta_l L_{l1}^{\mathrm{T}}\mathrm{diag}\{b_l\} \\ \delta_2\mathrm{diag}\{b_2\}L_{21} & \delta_2(\mathrm{diag}\{b_2\}L_{22} + L_{22}^{\mathrm{T}}\mathrm{diag}\{b_2\}) & \cdots & \delta_l L_{l2}^{\mathrm{T}}\mathrm{diag}\{b_l\} \\ \vdots & \vdots & \ddots & \vdots \\ \delta_l\mathrm{diag}\{b_l\}L_{l1} & \delta_l\mathrm{diag}\{b_l\}L_{l2} & \cdots & \delta_l(\mathrm{diag}\{b_l\}L_{ll} + L_{ll}^{\mathrm{T}}\mathrm{diag}\{b_l\}) \end{bmatrix} \tag{31}$$

On the other hand, taking the derivative of V_{z_i} defined in (35), and then using (22), we have

$$\begin{aligned} \nabla V_{z_i}\dot{z}_i &= \frac{1}{2}(\dot{z}_i^{\mathrm{T}} z_i + z_i^{\mathrm{T}}\dot{z}_i) \qquad (39)\\ &= \frac{1}{2}\Big(\big(f_i(x_i,v_i) + \mu_i + (a_i + \sum_{j\in N_i}\alpha_{ji})z_i - \sum_{j\in N_i}\alpha_{ji}z_j \\ &\quad -\big\{(L_{\mathcal{G}_c} + \mathrm{diag}\{a\})_i^2 \otimes I_n\big\}\bar{x}\big)^{\mathrm{T}} z_i + z_i^{\mathrm{T}}\big(f_i(x_i,v_i) \\ &\quad +\mu_i + (a_i + \sum_{j\in N_i}\alpha_{ji})z_i - \sum_{j\in N_i}\alpha_{ji}z_j \\ &\quad -\big\{(L_{\mathcal{G}_c} + \mathrm{diag}\{a\})_i^2 \otimes I_n\big\}\bar{x}\big)\Big) \\ &\le z_i^{\mathrm{T}}\big(\mu_i + (a_i + \sum_{j\in N_i}\alpha_{ji})z_i\big) \\ &\quad +|z_i|(\sum_{j\in N_i}\alpha_{ji}|z_j| + |\hat{L}_{2a_i}||\bar{x}| + |f_i(x_i,v_i)|). \end{aligned}$$

When $V_{z_i} \ge \max_{j\in N_i}\left\{\gamma_{z_i}^{\bar{x}}(V_{\bar{x}}), \gamma_{z_i}^{z_j}(V_{z_j})\right\}$, from the definitions of $V_{\bar{x}}$, V_{z_i}, $\gamma_{z_i}^{\bar{x}}$ and $\gamma_{z_i}^{z_j}$ ($i = 1,\ldots,N$ and $j \in N_i$), we obtain that

$$|\bar{x}| \le \rho_{\bar{x}}^{z_i}(|z_i|) \tag{40}$$

$$|z_j| \le \rho_{z_j}^{z_i}(|z_i|), \quad j \in N_i. \tag{41}$$

By substituting the control law μ_i in (33) into (39), and then considering (8), (40), and (41), it is achieved that

$$\nabla V_{z_i}\dot{z}_i \le -\frac{\sigma_{z_i}}{2} z_i^T z_i = -\sigma_{z_i} V_{z_i}$$

which indicates that V_{z_i} satisfying

$$V_{z_i} \ge \max_{j\in N_i}\left\{\gamma_{z_i}^{\bar{x}}(V_{\bar{x}}), \gamma_{z_i}^{z_j}(V_{z_j})\right\} \Rightarrow \nabla V_{z_i}\dot{z}_i \le -\sigma_{z_i} V_{z_i}. \tag{42}$$

Finally, let us investigate the $[\bar{x}^T, z_1^T, \ldots, z_N^T]^T$-system composed of (21), (22), and (33). As the ISS-Lyapunov functions $V_{\bar{x}}$ and V_{z_i} satisfying conditions (38) and (42), according to the cyclic-small-gain theorem provided in Lemma 5, the $[\bar{x}^T, z_1^T, \ldots, z_N^T]^T$-system is ISS if the cyclic-small-gain conditions (23)–(25) hold. Moreover, the ISS system is an unforced system because control law μ_i is designed. It is known that the ISS of an unforced system leads to the globally asymptotical stability [36], which means that the $[\bar{x}^T, z_1^T, \ldots, z_N^T]^T$-system is globally asymptotically stable, i.e.

$$\lim_{t\to\infty}\bar{x}(t) = \mathbf{0} \tag{43}$$

$$\lim_{t\to\infty} z(t) = \mathbf{0}. \tag{44}$$

From (12), and together with (43), we know $\lim_{t\to\infty} x_j(t) - p_j - x_d = 0$, for $j = 1,\ldots,N$. Correspondingly, for any $0 < j \ne i \le N$, we have $\lim_{t\to\infty}|x_j(t) - x_i(t) - (p_i - p_j)| = 0$ and $\lim_{t\to\infty} x_c(t) - x_d = \frac{1}{N}\sum_{i=1}^{N}\big(\lim_{t\to\infty} x_i(t) - p_i - x_d\big) = 0$.

From (44), and together with the definition of z, we obtain

$$\lim_{t\to\infty} v(t) = -(L_{\mathcal{G}_c} + \mathrm{diag}\{a\}) \otimes I_n \lim_{t\to\infty}\bar{x}(t) = \mathbf{0}.$$

So, the position center of multiagent system follows the virtual leader x_d, the positions of the agents converge to the prespecified geometric pattern $\mathcal{P}$, and the velocities converge to zero, i.e., the result in Theorem 1 is concluded. ■

Remark 5: It is worth noting that Theorem 1 shows that there are no requirements imposed on $\mathcal{G}_c$, the digraph depicting the information interconnection topology among all the N agents. It shows that an sufficient condition for the control law design is that $\mathcal{G}_c'$ has a spanning tree, which indicates according to [42] that at least one of the agents in each strongly connected component with zero in-degree should be informed in any information structure for guaranteeing the multiagent systems to arrive at the virtual leader with prespecified geometric pattern. As such, we only need to select one agent in each of the strongly connected component in $\mathcal{G}_c$ which is with zero in-degree. Obviously, the least number of agents which should be informed by the virtual leader in order to realize the coordinated behavior, is just the number of the strongly connected components with zero in-degree in $\mathcal{G}_c$. More illustrative details can be found in the example in the following subsection.

C. Examples and Simulation Results

We employ the six-agent system with $\mathcal{G}_c$ in Fig. 1 as an example to demonstrate the effectiveness of the control law proposed in Theorem 1.

For $i = 1,\ldots,6$, the dynamics of the ith agent is assumed to be

$$\dot{x}_i = v_i, \tag{45}$$

$$\dot{v}_i = u_i + f_i(v_i), \tag{46}$$

where $x_i, v_i, u_i \in \mathbb{R}^2$ and $f_i(v_i) = [v_{i1}^2; v_{i2}^2]$. Note that $f_i(v_i)$ does not satisfy the global Lipschitz condition.

Comparing the dynamics (46) with (1), we can take

$$\psi_{f_i}^{x_i}(|x_i|) = 0 \quad \text{and} \quad \psi_{f_i}^{v_i}(|v_i|) = |v_i|^2.$$

There are three strongly connected components in $\mathcal{G}_c$, labeled, respectively, by $\mathcal{G}_1$, $\mathcal{G}_2$ and $\mathcal{G}_3$ in Fig. 3. Clearly, the in-degree of $\mathcal{G}_3$ is 1 and the in-degrees of $\mathcal{G}_1$ and $\mathcal{G}_2$ are both zero, therefore according to the result in Theorem 1 and the discussions in Remark 5, there should be at least one node in each of $\mathcal{G}_1$ and $\mathcal{G}_2$ which is required to have access to the state information of the node 0 to guarantee the stability of the proposed control law and to realize the coordinated behavior, and thus the least number of agents which should be informed in this example is 2.

It is easy to obtain that $b_1 = [\frac{1}{3}, \frac{1}{3}, \frac{1}{3}]^T$, $b_2 = 1$ and $b_3 = [\frac{1}{2}, \frac{1}{2}]^T$. Simply choosing $\delta_2 = \delta_3 = 1$, inequality (32) can

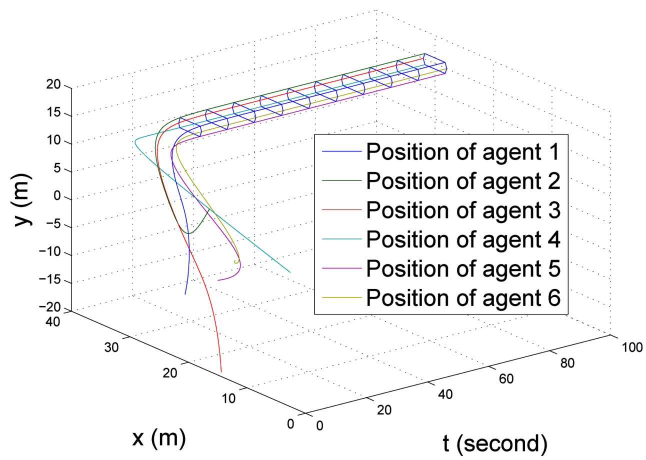

Fig. 4. Evolutions of the positions under control law (47).

be guaranteed; therefore, from Remark 4, the positive column vector $c = [\frac{1}{3}, \frac{1}{3}, \frac{1}{3}, 1, \frac{1}{2}, \frac{1}{2}]^T$ is obtained. Correspondingly, we have $\lambda_{\min}(\hat{L}_{ca}) = 0.0731$. After choosing $\epsilon = 0.031$, we obtain $\gamma_{\bar{x}}^{z_i}(s) = 1224.5\ s$ for $i = 1, \ldots, 6$. And further it is obtained that $|\hat{L}_{2a_1}| = 4.2426$, $|\hat{L}_{2a_2}| = |\hat{L}_{2a_3}| = 1.5$, $|\hat{L}_{2a_4}| = 1.8708$, $|\hat{L}_{2a_5}| = 6.0208$ and $|\hat{L}_{2a_6}| = 3.6401$.

There exist 6 nodes, 10 directed paths and 2 directed circles in $\mathcal{G}_c$ in Fig. 1. Specifically, the directed paths are $P = \{(1, 2), (2, 3), (3, 1), (4, 5), (5, 6), (6, 5), (1, 2, 3), (2, 3, 1), (3, 1, 2), (4, 5, 6)\}$ and the directed cycles are $C = \{(1, 2, 3, 1), (5, 6, 5)\}$. Correspondingly, there are 18 different inequalities in (23)–(25). From the discussions in Remark 3, to satisfy all the ISS cyclic-small-gain conditions, we can take $\gamma_{z_j}^{z_i}(s) = 0.9s$ for $(i, j) \in \mathcal{E}$ and $\gamma_{z_i}^{\bar{x}}(s) = 0.0008s$ for $i = 1, \ldots, 6$. Accordingly, we obtain $\rho_{\bar{x}}^{z_i}(s) = \tau^{-1} \circ \left(\gamma_{z_i}^{\bar{x}}\right)^{-1} \circ c_{\min}^{-1} \circ \tau(s) = 61.2372s$ and $\rho_{z_j}^{z_i}(s) = \tau^{-1} \circ \left(\gamma_{z_i}^{z_j}\right)^{-1} \circ \tau(s) = 1.0541s$. After taking $\sigma_{z_i} = 1$, the input for each agent is

$$\begin{cases} u_1 = -\frac{z_1}{|z_1|}(|v_1|^2 + 260.8590|z_1|) - 2.5z_1 \\ u_2 = -\frac{z_2}{|z_2|}(|v_2|^2 + 92.9099|z_2|) - 1.5z_2 \\ u_3 = -\frac{z_3}{|z_3|}(|v_3|^2 + 92.9099|z_3|) - 1.5z_3 \\ u_4 = -\frac{z_4}{|z_4|}(|v_4|^2 + 114.5626|z_4|) - 1.5z_4 \\ u_5 = -\frac{z_5}{|z_5|}(|v_5|^2 + 370.8051|z_5|) - 2.5z_5 \\ u_6 = -\frac{z_6}{|z_6|}(|v_6|^2 + 223.9636|z_6|) - 1.5z_6 \end{cases} \tag{47}$$

where $z_1 = v_1 + (x_1 - p_1 - x_d) + \big((x_1 - x_3) - (p_1 - p_3)\big) z_2 = v_2 + \big((x_2 - x_1) - (p_2 - p_1)\big) z_3 = v_3 + \big((x_3 - x_2) - (p_3 - p_2)\big) z_4 = v_4 + (x_4 - p_4 - x_d) z_5 = v_5 + \big((2x_5 - x_4 - x_6) - (2p_5 - p_4 - p_6)\big) z_6 = v_6 + \big((x_6 - x_5) - (p_6 - p_5)\big)$.

The prespecified geometric pattern is set to be a hexagon, that is $\mathcal{P} = \{(-\sqrt{3}, 1), (\sqrt{3}, 1), (2, 0), (\sqrt{3}, -1), (-\sqrt{3}, -1), (-2, 0)\}$. The initial positions for agents are $(20.6, -8.1)$, $(16.4, 9.2)$, $(14.4, -19.2)$, $(2.6, 4.1)$, $(15, -3)$, and $(12, 2)$, and the virtual leader is set to be $x_d = (30, 15)$. We then simulate the six-agent system with control law (47). The simulation results are shown in Figs. 4–7.

It is shown from Fig. 4 that the positions of all agents converge to a hexagon, i.e., the prespecified geometric pattern $\mathcal{P}$, and from Fig. 5 that the position center of all the agents converges to the center of the hexagon. The state error of the formation, defined by $e(t) = \sum_{i=1}^{5} |(x_i(t) - x_{i+1}(t)) - (p_i - p_{i+1})|$, converges to zero as that shown in Fig. 6. And further, the velocities on x and y directions for each agent are shown in Fig. 7(a) and Fig. 7(b), respectively. Obviously, they all converge to zeros. Therefore, the flocking objective (9)–(11) is achieved.

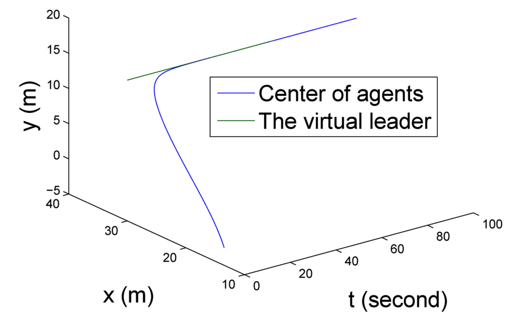

Fig. 5. Evolutions of the position center under control law (47).

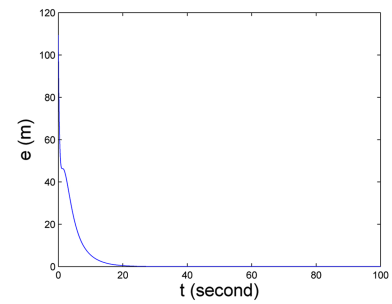

Fig. 6. Evolutions of formation error under control law (47).

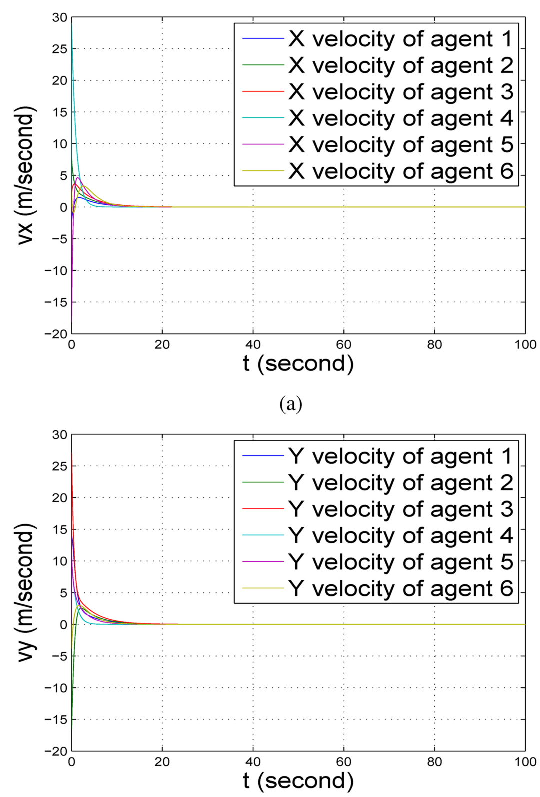

(a)

(b)

Fig. 7. Evolutions of the velocities under control law (47). (a) X velocities. (b) Y velocities.

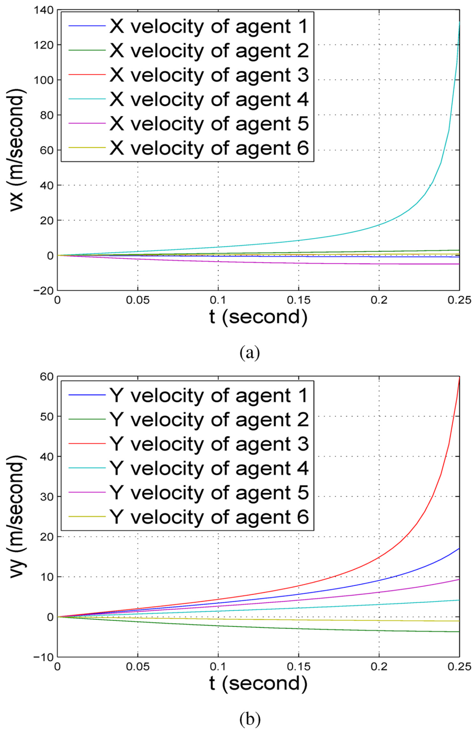

Fig. 8. Evolutions of the velocities under control law (48). (a) X velocities. (b) Y velocities.

For $i = 1, \ldots, 6$ and $j_i \in N_i$, if let $a_{1j_1} = 2.5$, $a_{2j_2} = 1.5$, $a_{3j_3} = 1.5$, $a_{4j_4} = 1.5$, $a_{5j_5} = 2.5$, $a_{5j_5} = 1.5$ and $k = -1$ in the widely used linear protocol in [19], then the linear protocol is specified as

$$\begin{cases} u_1 = -2.5z_1 \\ u_2 = -1.5z_2 \\ u_3 = -1.5z_3 \\ u_4 = -1.5z_4 \\ u_5 = -2.5z_5 \\ u_6 = -1.5z_6. \end{cases} \tag{48}$$

We simulate the above six-agent system with the linear protocol (48) and the same initial conditions as that for protocol (47). The velocity evolutions on x- and y-directions in 0.25 second interval are shown in Fig. 8, respectively. Clearly, the linear protocol (48) leads to divergence.

IV. Containment Control With Multiple Leaders

In this section, we will employ our technique to deal with another attractive coordination problem, the containment control of multiagent system.

A. System Descriptions

Different to the preceding section, we suppose in this section that there are $M - N$ $(M > N)$ virtual leaders labeled from agent $N+1$ to agent M for a group of N agents with dynamics (6)–(7); and the positions of these leaders are denoted by $x_i \in \mathbb{R}^n$ $(i = N+1, \ldots, M)$ accordingly. In the following, we denote $x_L = [x_{N+1}^T, \ldots, x_M^T]^T$, and employ $Co(x_L)$ to denote the convex hull spanned by x_L.

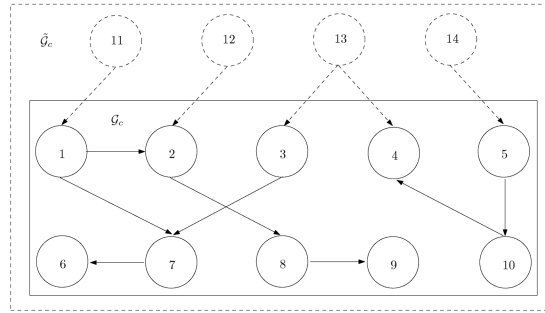

Fig. 9. $\mathcal{G}_c$ and $\tilde{\mathcal{G}}_c$ for a system with 10 agents and 4 leaders, in which nodes $i = \{1, \ldots, 10\}$ represent the agents and nodes $j = \{11, \ldots, 14\}$ represent the leaders.

We assume also that only a small part of the agents have access to the state information of a portion of the virtual leaders. To be more specific, we assume that

Assumption 2: For each of the N agents, there exists at least one virtual leader that has a directed path to the agent.

The main purpose of this section is to design a distributed control law μ_i for the ith $(i = 1, \ldots, N)$ agent, which uses only the position x_i, the velocity v_i and the state information of its neighbors (including the position information of the virtual leaders to which agent i has access), such that the position evolutions of the N agents asymptotically reach the convex hull $Co(x_L)$, i.e.

$$\lim_{t\to\infty} x_i(t) = \sum_{j=N+1}^{M} \epsilon_j x_j, \quad i = 1, \ldots, N = \tag{49}$$

where $0 \le \epsilon_j \le 1$ and $\sum_{j=N+1}^{M} \epsilon_j = 1$, and the velocities of N agents asymptotically converge to zero, i.e.

$$\lim_{t\to\infty} v_i(t) = 0. \tag{50}$$

B. Control Law Design

In the sequel, we will develop a nonlinear control law to make the N agents to achieve (49) and (50).

1) *Two-Cascade Model:* The information-interconnection digraph $\mathcal{G}_c$ is used to model the interconnection of N agents; and similarly the virtual information-interconnection digraph, described by $\tilde{\mathcal{G}}_c$ can be constructed by taking each agent (including N agents and $M - N$ leaders) as a node, and each existing directed interconnection between M agents as a directed edge. Correspondingly, the $\tilde{\mathcal{G}}_c$ for a system with 10 agents and 4 leaders is shown as an example in Fig. 9. It should be noted that if there is only one leader, then Assumption 2 is equivalent to that $\tilde{\mathcal{G}}_c$ has a spanning tree.

The following Lemma is summarized from [44] for providing some properties of $L_{\tilde{\mathcal{G}}_c}$, the Laplacian of $\tilde{\mathcal{G}}_c$.

Lemma 8: The Laplacian of $\tilde{\mathcal{G}}_c$ associated with N agents and $M - N$ leaders can be written as the block matrix

$$L_{\tilde{\mathcal{G}}_c} = \begin{bmatrix} L_1 & L_2 \\ \mathbf{0}_{(M-N)\times N} & \mathbf{0}_{(M-N)(M-N)} \end{bmatrix}, \tag{51}$$

where $L_1 \in \mathbb{R}^{N\times N}$ and $L_2 \in \mathbb{R}^{N(M-N)}$.

Evermore, if Assumption 2 holds, then

1) L_1 is a nonsingular matrix, and all eigenvalues of L_1 have positive real parts,
2) each entry of $-L_1^{-1}L_2$ is nonnegative and all row sums of $-L_1^{-1}L_2$ equal to one.

Considering L_1 is nonsingular, we denote $x_F = [x_1^T, \ldots, x_N^T]^T$, and

$$\bar{x}_F \triangleq x_F + (L_1^{-1}L_2 \otimes I_n)x_L. \tag{52}$$

For $i = 1, \ldots, N$, we define

$$v_i^* = \sum_{j=1}^{M} \alpha_{ij}(x_j - x_i) \tag{53}$$

where α_{ij} is the ijth element of the weighted adjacency matrix of $\tilde{\mathcal{G}}_c$.

Define $v_F^* = [v_1^{*T}, \ldots, v_N^{*T}]^T$. Then, from (53) and (51), and then using (52), we have

$$\begin{aligned} v_F^* &= -(L_1 \otimes I_n)\, x_F - (L_2 \otimes I_n)\, x_L \\ &= -(L_1 \otimes I_n)\, \bar{x}_F. \end{aligned} \tag{54}$$

Denote $v_F = [v_1^T, \ldots, v_N^T]^T$ and $z_F = [z_1^T, \ldots, z_N^T]^T = v_F - v_F^*$. It then follows directly from (6), (52) and (54) that

$$\dot{\bar{x}}_F = \dot{x}_F = z_F - (L_1 \otimes I_n)\, \bar{x}_F. \tag{55}$$

Further, differentiating both sides of (54), we have

$$\dot{v}_F^* = -(L_1 \otimes I_n)\dot{\bar{x}}_F. \tag{56}$$

By substituting $\dot{\bar{x}}_F$ in (55) into (56) yields

$$\dot{v}_F^* = -(L_1 \otimes I_n)\Big(z_F - (L_1 \otimes I_n)\bar{x}_F\Big). \tag{57}$$

Then, differentiating both sides of $z_F = v_F - v_F^*$ and using (57), we have

$$\dot{z}_F = \dot{v}_F + (L_1 \otimes I_n)z_F - (L_1 \otimes I_n)^2\bar{x}_F. \tag{58}$$

Consequentially, for $i = 1, \ldots, N$, by using (6), (7), together with (55) and (58), the two-cascade model is summarized as follows:

$$\dot{\bar{x}}_F = z_F - (L_1 \otimes I_n)\, \bar{x}_F \tag{59}$$

$$\dot{z}_i = \mu_i + f_i(x_i, v_i) + \sum_{j=1}^{M} \alpha_{ij} z_i - \sum_{j\in N_i} (\alpha_{ij} z_j) - (L_1 \otimes I_n)_i^2 \bar{x}_F \tag{60}$$

where N_i are the neighbors of node i in $\mathcal{G}_c$, and $(L_1 \otimes I_n)_i^2$ is the ith row of $(L_1 \otimes I_n)^2$. Also, cascade 1 described by (59) and cascade 2 described by (60) are called $\bar{x}_F$-subsystem and z_i-subsystems in the following, respectively.

Similarly, considering the states $\bar{x}_F$ and z_i as nodes, and the gain connections between states as directed edges, the interconnected system composed of the $\bar{x}_F$-subsystem and the z_i-subsystems can be modeled by the gain-interconnection digraph $\mathcal{G}_g$ too. Fig. 10 shows the corresponding $\mathcal{G}_g$ of the $\mathcal{G}_c$ modeled by Fig. 9.

It is clear that the cyclic-small-gain conditions discussed in Section III-B are compatible with the gain-interconnection

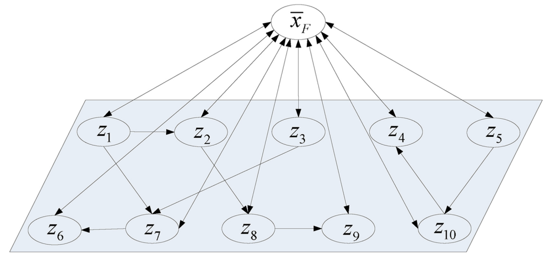

Fig. 10. Gain-interconnection digraph of the system with 10 agents and 4 leaders.

digraph built in this section, that is to say the cyclic-small-gain conditions required by Lemma 4 can be specified by inequalities (23)–(25) too.

2) *Main Result:* It is known that all eigenvalues of L_1 have positive real parts if Assumption 2 holds, therefore according to Lemma 2, there exists a positive definite matrix $P \in \mathbb{R}^{N\times N}$ such that $PL_1 + L_1^T P > 0$. Denote the minimum eigenvalue of the positive definite matrix P by $\lambda_{\min}(P) > 0$.

Theorem 2: For a group of N agents with dynamics (6)–(7) and Assumption 1, if Assumption 2 and the cyclic-small-gain conditions (23)–(25) resulting from its corresponding $\mathcal{G}_g$ hold then under control law

$$\mu_i = \begin{cases} -\frac{z_i}{|z_i|}\mu_i' - \left(\frac{\sigma_{z_i}}{2} + \sum_{j=1}^{M} \alpha_{ji}\right) z_i, & \text{when } z_i \neq 0 \\ 0, & \text{when } z_i = 0 \end{cases} \tag{61}$$

where

$$\mu_i' = \psi_{f_i}^{x_i}(|x_i|) + \psi_{f_i}^{v_i}(|v_i|) + |(L_1 \otimes I_n)_i^2| \rho_{\bar{x}}^{z_i}(|z_i|) + \sum_{j\in N_i} \alpha_{ij}\rho_{z_j}^{z_i}(|z_i|)$$

and $\sigma_{z_i} > 0$ is an arbitrary positive real constant, $\rho_{\bar{x}}^{z_i}(s) = \tau^{-1} \circ \left(\gamma_{z_i}^{\bar{x}}\right)^{-1} \circ \lambda_{\min}^{-1}(P) \circ \tau(s)$ and $\rho_{z_j}^{z_i}(s) = \tau^{-1} \circ \left(\gamma_{z_i}^{z_j}\right)^{-1} \circ \tau(s)$ with functions $\gamma_{z_i}^{\bar{x}}$ and $\gamma_{z_i}^{z_j}$ for $j \in N_i$ are any functions of class $\mathcal{K}_\infty$ and $\tau(s) = \frac{1}{2}s^2$, the containment control of the N agents can be guaranteed finally, namely the control objective described by (49) and (50) is achieved.

Proof: We define the ISS-Lyapunov function candidates for the $\bar{x}_F$-subsystem in (59) and z_i-subsystems in (60), respectively, as follows:

$$V_{\bar{x}_F}(\bar{x}_F) = \frac{1}{2}\bar{x}_F^{\mathrm{T}}(P \otimes I_n)\bar{x}_F, \tag{62}$$

$$V_{z_i}(z_i) = \tau(|z_i|), \quad i = 1, \ldots, N. \tag{63}$$

In the following discussions, $V_{\bar{x}_F}$ and V_{z_i} are simply used instead of $V_{\bar{x}_F}(\bar{x}_F)$ and $V_{z_i}(z_i)$, respectively.

Denote the minimum eigenvalue of the positive definite matrix $\frac{1}{2}(L_1^T P + PL_1)$ and the maximum eigenvalue of the positive definite matrix P by $\lambda_{\min}(L_1 P) > 0$ and $\lambda_{\max}(P) > 0$, respectively. Considering any positive $0 < \epsilon < \lambda_{\min}(L_1 P)$, we define a function of class $\mathcal{K}_\infty$ as

$$\gamma_{\bar{x}}^{z_i}(s) = N\lambda_{\max}(P)\left(\frac{\lambda_{\max}(P)}{\lambda_{\min}(L_1 P) - \epsilon}\right)^2 s, \quad \forall s \in \mathbb{R}_+$$

and then with the similar tricks in the proof of theorem 1, it can be obtained that

$$V_{\bar{x}_F} \geq \max_{i=1,\dots,N} \left\{\gamma_{\bar{x}}^{z_i}(V_{z_i})\right\} \Rightarrow \nabla V_{\bar{x}_F}\dot{\bar{x}}_F \leq -\frac{2\epsilon}{\lambda_{\max}(P)}V_{\bar{x}_F} \quad (64)$$

$$V_{z_i} \geq \max_{j\in N_i} \left\{\gamma_{z_i}^{\bar{x}}(V_{\bar{x}_F}), \gamma_{z_i}^{z_j}(V_{z_j})\right\} \Rightarrow \nabla V_{z_i}\dot{z}_i \leq -\sigma_{z_i}V_{z_i}. \quad (65)$$

Consequentially, as the ISS-Lyapunov functions $V_{\bar{x}_F}$ and V_{z_i} satisfying conditions (64) and (65), according to the cyclic-small-gain theorem provided in Lemma 5, if the cyclic-small-gain conditions (23)–(25) hold, then the $[\bar{x}_F^T, z_1^T, \dots, z_N^T]^T$-system composed of (59), (60), and (61) is globally asymptotically stable, i.e.

$$\lim_{t\to\infty} \bar{x}_F(t) = \mathbf{0} \quad (66)$$

$$\lim_{t\to\infty} z(t) = \mathbf{0}. \quad (67)$$

From (52) and (66), we have

$$\lim_{t\to\infty} x_F(t) = (-L_1^{-1}L_2)x_L.$$

According to Lemma 8 that each entry of $-L_1^{-1}L_2$ is nonnegative and all row sums of $-L_1^{-1}L_2$ equal to one, and then from the definition of convex hull in Definition 1, it is known that x_F will converge to $Co(x_L)$.

On the other hand, from (67) and the definition of z, it follows that $\lim_{t\to\infty} v(t) = \mathbf{0}$.

Therefore, the positions of the N agents will converge to the convex hull spanned by the positions of the $M-N$ leaders, and their velocities will converge to zero, i.e., the result in Theorem 2 is concluded. ■

C. Examples and Simulation Results

We employ the multiagent system with $\tilde{\mathcal{G}}_c$ in Fig. 9 as an example to demonstrate the effectiveness of the control law proposed in Theorem 2.

For $i = 1, \dots, 10$, the dynamics of the ith agent is assumed to be (45) and (46) too, and we also take $\psi_{f_i}^{x_i}(|x_i|) = 0$ and $\psi_{f_i}^{v_i}(|v_i|) = |v_i|^2$. Taking all the weights of the directed edges as 1, then the Laplacian of $\tilde{\mathcal{G}}_c$ is

$$L_{\tilde{\mathcal{G}}_c} = \begin{bmatrix} L_1 & L_2 \\ \mathbf{0}_{4\times 10} & \mathbf{0}_{4\times 4}\end{bmatrix}$$

where

$$L_1 = \begin{bmatrix} 1 & 0 & 0 & 0 & 0 & 0 & 0 & 0 & 0 & 0 \\ -1 & 2 & 0 & 0 & 0 & 0 & 0 & 0 & 0 & 0 \\ 0 & 0 & 1 & 0 & 0 & 0 & 0 & 0 & 0 & 0 \\ 0 & 0 & 0 & 2 & 0 & 0 & 0 & 0 & 0 & -1 \\ 0 & 0 & 0 & 0 & 1 & 0 & 0 & 0 & 0 & 0 \\ 0 & 0 & 0 & 0 & 0 & 1 & -1 & 0 & 0 & 0 \\ -1 & 0 & -1 & 0 & 0 & 0 & 2 & 0 & 0 & 0 \\ 0 & -1 & 0 & 0 & 0 & 0 & 0 & 1 & 0 & 0 \\ 0 & 0 & 0 & 0 & 0 & 0 & 0 & -1 & 1 & 0 \\ 0 & 0 & 0 & 0 & -1 & 0 & 0 & 0 & 0 & 1 \end{bmatrix}$$

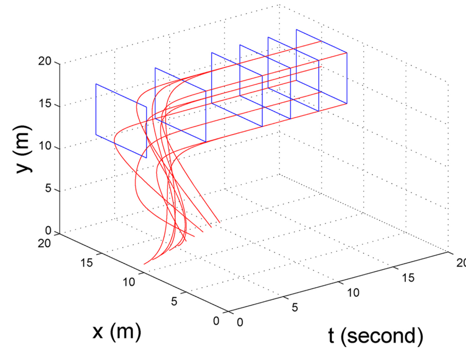

Fig. 11. Position evolutions of ten agents (red) and four leaders (blue).

$$L_2 = \begin{bmatrix} -1 & 0 & 0 & 0 \\ 0 & -1 & 0 & 0 \\ 0 & 0 & -1 & 0 \\ 0 & 0 & -1 & 0 \\ 0 & 0 & 0 & -1 \\ 0 & 0 & 0 & 0 \\ 0 & 0 & 0 & 0 \\ 0 & 0 & 0 & 0 \\ 0 & 0 & 0 & 0 \\ 0 & 0 & 0 & 0 \end{bmatrix}. \quad (68)$$

Simply letting $PL_1^T + L_1P = I_{10\times 10}$, the positive define matrix P is obtained, and consequentially we obtain $\lambda_{\max}(P) = 1.2046$, $\lambda_{\min}(P) = 0.1999$ and $\lambda_{\min}(L_1P) = 0.5$. Taking $\epsilon = 0.1$ in (64), we obtain $\gamma_{\bar{x}}^{z_i}(s) = 109.2468s$. From the discussions in Remark 3, to satisfy all the ISS cyclic-small-gain conditions, we can take $\gamma_{z_j}^{z_i}(s) = 0.9s$ for $(i, j) \in \mathcal{E}$ and $\gamma_{z_i}^{\bar{x}}(s) = 0.009s$ for $i = 1, \dots, 10$. Accordingly, we obtain $\rho_{\bar{x}}^{z_i}(s) = \tau^{-1} \circ \left(\gamma_{z_i}^{\bar{x}}\right)^{-1} \circ \lambda_{\min}^{-1}(P) \circ \tau(s) = 23.5761s$ and $\rho_{z_j}^{z_i}(s) = \tau^{-1} \circ \left(\gamma_{z_i}^{z_j}\right)^{-1} \circ \tau(s) = 1.0541s$. After taking $\sigma_{z_i} = 1$ in (61), the input for each agent is

$$\begin{cases} u_1 = -\frac{z_1}{|z_1|}(|v_1|^2 + 108.0398|z_1|) - 1.5z_1 \\ u_2 = -\frac{z_2}{|z_2|}(|v_2|^2 + 121.2686|z_2|) - 2.5z_2 \\ u_3 = -\frac{z_3}{|z_3|}(|v_3|^2 + 78.1925|z_3|) - 1.5z_3 \\ u_4 = -\frac{z_4}{|z_4|}(|v_4|^2 + 95.3585|z_4|) - 2.5z_4 \\ u_5 = -\frac{z_5}{|z_5|}(|v_5|^2 + 57.7497|z_5|) - 1.5z_5 \\ u_6 = -\frac{z_6}{|z_6|}(|v_6|^2 + 24.6302|z_6|) - 1.5z_6 \\ u_7 = -\frac{z_7}{|z_7|}(|v_7|^2 + 119.9887|z_7|) - 2.5z_7 \\ u_8 = -\frac{z_8}{|z_8|}(|v_8|^2 + 53.7726|z_8|) - 1.5z_8 \\ u_9 = -\frac{z_9}{|z_9|}(|v_9|^2 + 109.0939|z_9|) - 1.5z_9 \\ u_{10} = -\frac{z_{10}}{|z_{10}|}(|v_{10}|^2 + 109.0939|z_{10}|) - 1.5z_{10}, = \end{cases} \quad (69)$$

where $z_1 = v_1 + (x_1 - x_{11})$, $z_2 = v_2 + (x_2 - x_1) + (x_2 - x_{12})$, $z_3 = v_3+(x_3-x_{13})z_4 = v_4+(x_4-x_{13})+(x_4-x_{10})z_5 = v_5+(x_5-x_{14})z_6 = v_6+(x_6-x_7)z_7 = v_7+(x_7-x_1)+(x_7-x_3)z_8 = v_8+(x_8-x_2)z_9 = v_9+(x_9-x_8)z_{10} = v_{10}+(x_{10}-x_5)$.

The initial positions of N agents are set to be (1, 10), (2, 9), (3, 8), (4, 7), (5, 6), (6, 5), (7, 4), (8, 3) (9, 2) and (10, 1), and the positions of the leaders are set to be (12, 18), (18, 18), (18, 12), (12, 12). We then simulate the multiagent system with control law (69). The simulation results are shown in Figs. 11–13.

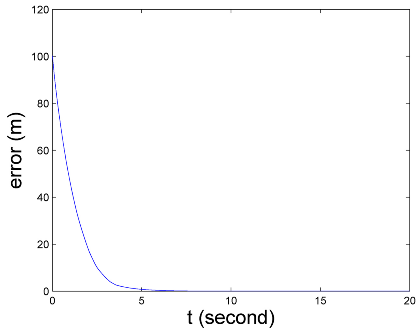

Fig. 12. Evolutions of containment errors under control law (61).

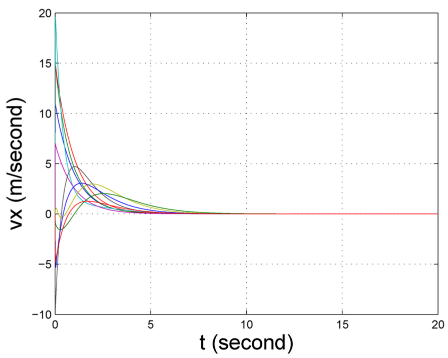

(a)

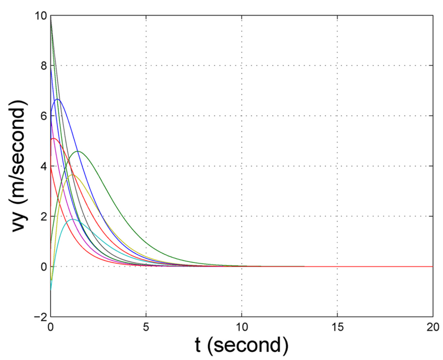

(b)

Fig. 13. Velocity evolutions of ten agents under control law (61). (a) X velocities. (b) Y velocities.

It is shown from Fig. 11 that the positions of all ten agents converge to the convex hull spanned by the positions of four leaders. The containment errors of the formation, defined by the sum of the distance between each agent and the spanned convex hull, converge to zero as that shown in Fig. 12. Further, the velocities on x and y directions for each agent are shown in Fig. 13 (a) and (b), respectively. Obviously, they all converge to zero. Therefore, the objective for containment control (49)–(50) is achieved.

V. Conclusion

Distributed control strategies for coordination problems, i.e., flocking with a virtual leader and containment control for multiagent systems with second-order locally Lipschitz continuous nonlinear dynamics under directed interaction topology are developed in this paper though a new approach, which is a blend of graph theory, ISS cyclic-small-gain theorem and backstepping techniques. Due to the considered locally Lipschitz continuous nonlinear dynamics for each isolated agent, the techniques performed in most existing works regarding nonlinear dynamics, which are intrinsically for its approximated linear counterpart under globally Lipschtiz continuous condition, cannot be extended to deal with the coordination problems in this paper. However, the newly proposed strategies can effectively tackle the technical challenges caused by the locally Lipschitz continuous nonlinear dynamics. And it is proved that only a portion of the agents having access to the state information of the leader(s) can guarantee the coordinated behaviors successfully with the proposed strategies.

It is worthy of mentioning that the case that the leaders are moving with varying velocities is an interesting topic which deserves further investigation. Furthermore, nonlinear multiagent systems with more complex factors, such as the external disturbances, switching topology, and time-delay, deserve deep investigate in our future work.

References

[1] R. W. Beard, J. Lawton, and F. Y. Hadaegh, "A coordination architecture for spacecraft formation control," *IEEE Trans. Control Syst. Technol.*, vol. 9, no. 6, pp. 777–790, Nov. 2001.

[2] Z. Lin, B. Francis, and M. Maggiore, "Necessary and sufficient graphical conditions for formation control of unicycles," *IEEE Trans. Autom. Control*, vol. 50, no. 1, pp. 121–127, Jan. 2005.

[3] B. D. Anderson, C. Yu, B. Fidan, and J. M. Hendrickx, "Rigid graph control architecture for autonomous formation," *IEEE Control Syst. Mag.*, vol. 28, no. 6, pp. 48–63, Dec. 2008.

[4] W. Dong and J. A. Farrell, "Cooperative control of multiple nonholonomic mobile agents," *IEEE Trans. Autom. Control*, vol. 53, no. 6, pp. 1434–1448, Jul. 2008.

[5] T. Vicsek, A. Czirook, E. Ben-Jacob, I. Cohen, and O. Shochet, "Novel type of phase transition in a system of self-deriven particles," *Phys. Rev. Lett.*, vol. 75, no. 6, pp. 1226–1229, 1995.

[6] S. G. Reeds, "Can a minority of informed leaders determine the foraging movements of a fish shoal?" *Animal Behav.*, vol. 59, no. 2, pp. 403–409, 2000.

[7] I. D. Couzin, J. Krause, N. R. Franks, and S. A. Levin, "Effective leadership and decision-making in animal groups on the move," *Nature*, vol. 433, no. 3, pp. 513–516, 2005.

[8] R. Olfati-Saber, "Flocking for multiagent dynamic systems: Algorithms and theory," *IEEE Trans. Autom. Control*, vol. 51, no. 3, pp. 401–420, Mar. 2006.

[9] H. Su, X. Wang, and Z. Lin, "Flocking of multi-agents with a virtual leader," *IEEE Trans. Autom. Control*, vol. 54, no. 2, pp. 293–307, Feb. 2009.

[10] H. G. Tanner, A. Jadbabaie, and G. J. Pappas, "Flocking in fixed and switching networks," *IEEE Trans. Autom. Control*, vol. 52, no. 5, pp. 863–868, May 2007.

[11] W. Dong, "Flocking of multiple mobile robots based on backstepping," *IEEE Trans. Syst., Man Cybern. B, Cybern.*, vol. 41, no. 2, pp. 414–424, Apr. 2011.

[12] W. Ren, W. Beard, and E. M. Atkins, "Information consensus in multivehicle cooperative control," *IEEE Control Syst. Mag.*, vol. 27, no. 2, pp. 71–82, Apr. 2007.

[13] J. A. Fax and R. M. Murray, "Information flow and cooperative control of vehicle formations," *IEEE Trans. Autom. Control*, vol. 49, no. 9, pp. 1465–1476, Sep. 2004.

[14] R. Olfati-Saber and R. M. Murray, "Consensus problems in networks of agents with switching topology and time-delays," *IEEE Trans. Autom. Control*, vol. 49, no. 9, pp. 1520–1553, Sep. 2004.

[15] Z. Lin, M. Broucke, and B. Francis, "Local control strategies for groups of mobile autonomous agents," *IEEE Trans. Autom. Control*, vol. 49, no. 4, pp. 622–629, Sep. 2004.

[16] W. Ren and R. Beard, "Consensus seeking in multiagent systems under dynamically changing interaction topologies," *IEEE Trans. Autom. Control*, vol. 50, no. 5, pp. 655–661, May 2005.

[17] M. Cao, A. S. Morse, and B. D. O. Anderson, "Reaching a consensus in a dynamically changing environment: A graphical approach," *SIAM J. Control Optimiz.*, vol. 47, no. 2, pp. 575–600, 2008.
[18] Y. Hong, L. Gao, D. Cheng, and J. Hu, "Lyapunov-based approach to multiagent systems with switching jointly connected interconnection," *IEEE Trans. Autom. Control*, vol. 52, no. 5, pp. 943–948, May 2007.
[19] G. Xie and L. Wang, "Consensus control for a class of networks of dynamic agents," *Int. J. Robust Nonlinear Control*, vol. 17, nos. 10–11, pp. 941–959, 2007.
[20] J. Qin, W. X. Zheng, and H. Gao, "Consensus of multiple second-order vehicles with a time-varying reference signal under directed topology," *Automatica*, vol. 47, no. 9, pp. 1983–1991, 2011.
[21] Y. Cao and W. Ren, "Distributed coordinated tracking with reduced interaction via a variable structure approach," *IEEE Trans. Autom. Control*, vol. 57, no. 1, pp. 33–48, Jan. 2012.
[22] Y. P. Tian and Y. Zhang, "High-order consensus of heterogeneous multi-agent systems with unknown communication delays," *Automatica*, vol. 48, no. 6, pp. 1205–1212, 2012.
[23] Y. Zhao, B. Li, J. Qin, H. Gao, and H. R. Karimi, "H_∞ consensus and synchronization of nonlinear systems based on a novel fuzzy model," *IEEE Trans. Cybern.*, vol. 43, no. 6, pp. 2157–2169, Dec. 2013.
[24] H. Li, X. Liao, and T. Huang, "Second-order locally dynamical consensus of multiagent systems with arbitrarily fast switching directed topologies," *IEEE Trans. Cybern.*, vol. 43, no. 6, pp. 1343–1353, Dec. 2013.
[25] W. Yu, G. Chen, M. Cao, and J. Kurths, "Second-order consensus for multiagent systems with directed topologies and nonlinear dynamics," *IEEE Trans. Syst. Man Cybern. B*, vol. 40, no. 3, pp. 881–891, Jun. 2010.
[26] Q. Song, J. Cao, and W. Yu, "Second-order leader-following consensus of nonlinear multi-agent systems via pinning control," *Syst. Control Lett.*, vol. 59, no. 9, pp. 553–562, 2010.
[27] Q. Song, F. Liu, J. Cao, and W. Yu, "M-matrix strategies for pinning-controlled leader-following consensus in multiagent systems with nonlinear dynamics," *IEEE Trans. Cybern.*, vol. 43, no. 6, pp. 1688–1697, Dec. 2013.
[28] A. Das and F. L. Lewis, "Cooperative adaptive control for synchronization of sencond-order systems with unknown nonlinearities," *Int. J. Robust Nonlinear Control*, vol. 21, no. 13, pp. 1509–1524, 2011.
[29] Y. Cao, D. Stuart, W. Ren, and Z. Meng, "Distributed containment control for multiple autonomous vehicles with double-integrator dynamics: Algorithms and experiments," *IEEE Trans. Control Syst. Technol.*, vol. 19, no. 4, pp. 929–938, Jul. 2011.
[30] J. Li, W. Ren, and S. Xu, "Distributed containment control with multiple dynamic leaders for double-integrator dynamics using only position measurements," *IEEE Transa. Autom. Control*, vol. 57, no. 6, pp. 1553–1559, Jun. 2012.
[31] Y. Lou and Y. Hong, "Target containment control of multi-agent systems with random switching interconnection topologies," *Automatica*, vol. 48, no. 5, pp. 879–885, 2012.
[32] J. Mei, W. Ren, and G. Ma, "Distributed containment control for Lagrangian networks with parametric uncertainties under a directed graph," *Automatica*, vol. 48, no. 4, pp. 653–659, 2012.
[33] Z. Meng, W. Ren, and Z. You, "Distributed finite-time attitude containment control for multiple rigid bodies," *Automatica*, vol. 46, no. 12, pp. 2092–2099, 2010.
[34] G. Shi, Y. Hong, and K. H. Johansson, "Connectivity and set tracking of multi-agent systems guided by multiple moving leaders," *IEEE Trans. Autom. Control*, vol. 57, no. 3, pp. 663–676, Mar. 2012.
[35] M. Krstić, I. Kanellakopoulos, and P. V. Kokotović, *Nonlinear and Adaptive Control Design*. New York, NY, USA: Wiley, 1995.
[36] E. D. Sontag, "Input to state stability: Basic concepts and results," in *Nonlinear and Optimal Control Theory*, P. Nistri and G. Stefani, Eds. Berlin, Germany: Springer-Verlag, 2007, pp. 163–220.
[37] S. Dashkovskiy, B. S. Rüffer, and F. R. Wirth, "Small gain theorems for large scale systems and construction of ISS Lyapunov functions," *SIAM J. Control Optimiz.*, vol. 48, no. 6, pp. 4089–4118, 2010.
[38] T. Liu, D. J. Hill, and Z. P. Jiang, "Lyapunov formulation of ISS small-gain in continuous-time dynamical networks," *Automatica*, vol. 47, no. 9, pp. 2088–2093, 2011.
[39] C. Godsil and G. Royle, *Algebraic Graph Theory*. New York, NY, USA: Springer-Verlag, 2001.
[40] B. Boyd, L. E. Ghaoui, E. Feron, and V. Balakrishnan, *Linear Matrix Inequalities in Systems and Control Theory*. Philadelphia, PA, USA: SIAM, 1994.
[41] H. Minc, *Nonnegative Matrices*. New York, NY, USA: Wiley, 1988.
[42] J. Qin, W. X. Zheng, and H. Gao, "On pinning synchronisability of complex networks with arbitrary topological structure," *Int. J. Syst. Sci.*, vol. 42, no. 9, pp. 1559–1571, 2011.
[43] R. A. Brualdi and H. J. Ryser, *Combinatorial Matrix Theory*. Cambridge, U.K.: Cambridge Univ. Press, 1991.
[44] J. Mei, W. Ren, and G. Ma, "Distributed containment control for multiple nonlinear systems with identical dynamics," in *Proc. 30th Chin. Control Conf.*, 2011, pp. 6544–6549.

Xiangke Wang (M'12) received the B.S., M.S., and Ph.D. degrees from the National University of Defense Technology, Hunan, China, in 2004, 2006, and 2012, respectively.

He is currently a Lecturer with the College of Mechatronic Engineering and Automation, National University of Defense Technology. He was a visiting Ph.D student with the Research School of Engineering, the Australian National University, Canberra, Australia, supported by the China Scholarship Council from September 2009 to September 2011. His current research interests include coordination control of multiple UAV, nonlinear control, and robot soccer.

Jiahu Qin (M'12) received the B.S., M.S., and Ph.D. degrees from the Harbin Institute of Technology, Harbin, China, in 2003, 2005, and 2012, respectively.

He is currently a Research Fellow with the Research School of Engineering, Australian National University, Canberra, Australia. His current research interests include consensus problems in multiagent coordination and synchronization of complex dynamical networks

Changbin Yu (SM'10) received the B.Eng. degree (with first-class honors) in computer engineering from Nanyang Technological University, Nanyang, Singapore, in 2004, and the Ph.D. degree in information engineering from the Australian National University, Canberra, Australia, in 2008. Since 2008, he has been an Academic Staff Member with the Australian National University and also holding adjunct appointments with National ICT Australia, Canberra, and Shandong Computer Science Center, Shandong, China. His current research interests include the control of autonomous formations, multiagent systems, mobile sensor networks, human–robot interaction, and graph theory.

Dr. Yu was a recipient of the Australian Government Endeavor Asia Award in 2005, the Inaugural Westpac Australian Chinese Students New Age Award in 2006, the Chinese Government Outstanding Overseas Students Award in 2006, and the Asian Journal of Control Best Paper Award from 2006 to 2009. He won a competitive Australian Post-Doctoral Fellowship in 2007 and a prestigious Australian Research Council Queen Elizabeth II Fellowship (QEII) in 2010.